urban science

MDPI

Article

A Systematic Assessment of Greening Interventions for Developing Best Practices for Urban Heat Mitigation—The Case of Huế, Vietnam

Sebastian Scheuer [1,*], Luca Sumfleth [1], Long Dac Hoang Nguyen [2], Ylan Vo [2], Thi Binh Minh Hoang [2] and Jessica Jache [1]

[1] Landscape Ecology Lab, Geography Department, Humboldt-Universität zu Berlin, 10099 Berlin, Germany
[2] Mientrung Institute for Scientific Research, Vietnam National Museum of Nature, Vietnam Academy of Science and Technology, Huế 530000, Vietnam; hoangtbinhminh@vnmn.vast.vn (T.B.M.H.)
* Correspondence: sebastian.scheuer@geo.hu-berlin.de

Abstract: The health of urban populations is increasingly at risk due to the amplification and chronification of urban heat stress by climate change. This is particularly true for urban environments in humid tropical climates, including many cities in Southeast Asia. It is also in these locations where increasing climatic risks may be exacerbated by urban growth, underscoring the need to develop effective mitigation strategies for strengthening urban resilience and supporting climate change adaptation. Conservation and widespread implementation of green infrastructure (GI) are regarded as one means to counter heat as a public health threat. However, for lower-income countries across Southeast Asia, such as Vietnam, knowledge gaps remain with respect to the effectiveness of greening interventions for heat mitigation. To address this gap, in the context of urban expansion in the humid tropical city of Huế, Vietnam, diurnal cooling potential and regulation of outdoor thermal comfort (OTC) within a wide, shallow street canyon were systematically assessed for selected elements of GI along a quantitative and qualitative dimension using ENVI-met. Tree-based interventions were found to be most effective, potentially decreasing UTCI by −1.9 K at the domain level. Although lower in magnitude, green verges and green facades were also found to contribute to OTC, with green verges decreasing UTCI by up to −1.7 K and green facades by up to −1.4 K locally. Potential synergistic cooling impacts were identified through a combination of GI elements. However, no scenario was found to decrease heat stress to zero or moderate levels. Substantially reducing heat stress may thus require further measures and a closer consideration of local morphological characteristics.

Keywords: climate change adaptation; green infrastructure (GI); cooling potential; UTCI; outdoor thermal comfort (OTC); ENVI-met; Vietnam

Citation: Scheuer, S.; Sumfleth, L.; Nguyen, L.D.H.; Vo, Y.; Hoang, T.B.M.; Jache, J. A Systematic Assessment of Greening Interventions for Developing Best Practices for Urban Heat Mitigation—The Case of Huế, Vietnam. *Urban Sci.* **2024**, *8*, 67. https://doi.org/10.3390/urbansci8020067

Academic Editors: Aya Hagishima and Luis Hernández-Callejo

Received: 23 February 2024
Revised: 31 May 2024
Accepted: 6 June 2024
Published: 13 June 2024

1. Introduction

Increasing temperatures in cities, in combination with higher frequency and intensity of heatwaves, pose a major climate risk for the health and well-being of urban populations. For Vietnam, climate change and climate change-related hazards, i.e., extreme weather events, flooding, drought, the amplification and chronification of heat stress, the occurrence of vector-borne diseases, and increasing pressure on water resources, are seen as major threats to human health and well-being, livelihoods, economic assets, and ecosystems [1,2]. Against this background, greening measures and urban green infrastructure (GI) are seen as key to addressing these climate change risks by increasing the resilience of cities through protecting and promoting biodiversity, providing ecosystem services, and positively impacting the human, social, and natural capital of a city. In the context of urban heat, the focus here is particularly on their benefits for cooling and improvement of outdoor thermal comfort (OTC).

There is intensive research that recognizes GI, i.e., the interconnected, multifunctional, planned, or unplanned systems of natural and semi-natural GI elements, as effective greening strategies to increase urban resilience towards climate change impacts by shaping microclimatic conditions [3–7]. GI includes, e.g., urban green spaces, street greenery, green roofs, vertical greenery, and tree-based urban ecosystems. GI regulates air temperature, humidity, and solar radiation through shading, evaporative cooling, airflow modification, and heat exchange [8], thereby forming local urban cool islands to counter the urban heat island effect [7]. In so doing, GI modifies thermal sensation and perception and, thus, OTC [9]. However, widespread GI implementation is seen as crucial for the substantial mitigation of urban heat [3].

OTC is objectively regulated by the meteorological parameters solar radiation and, thus, mean radiant temperature, wind speed, air temperature, and relative humidity, but it is also driven by acclimatization, personal behavioral and psychological adaptation, expectations, activity level, or desire for exposure to sun or wind [10–13]. Mean radiant temperature, air temperature, and relative humidity were found to drive thermal discomfort (ibid.), whereas higher wind speed and shading, but also personal desire for more sunlight, improve subjective OTC [10]. OTC is also governed by frequent thermal alliesthesia, i.e., thermal transitions that drive, e.g., psychological thermal adaptation [9].

Typically, biophysical modeling is conducted to assess the impacts of different types of GI on meteorological parameters such as air temperature and OTC [5,6]. Often, individual (larger) green open spaces and tree canopies, or their joint realization, e.g., in the form of urban green spaces, woodlands, or forests, are the focus of study [5,14]. Increasingly, though, the focus of research shifts towards function- and benefit-mediating factors [15,16]. These mediating factors include (i) GI configuration, i.e., GI type, patch size, shape, density, and fragmentation; (ii) vegetation structure, i.e., plant species choice and composition, diversity, total vegetation coverage, planting conditions, and health of vegetation; (iii) urban morphology, including width or orientation of streets and density, shape, or height of surrounding built-up structures; and (iv) climate background, including wind speed and wind direction [5,6,16,17]. In this regard, it has been shown that street trees are highly effective in mitigating urban heat [7], and accordingly, an increase in tree canopy cover is reported as an effective cooling intervention [16], particularly in dense, high-compact cities [18,19]. In subtropical cities, street trees were found to provide cooling for most of the summer season, particularly during the early afternoon [20]. Planting patterns were shown to significantly affect the provided cooling and thermal comfort, with certain arrangements, e.g., double rows of trees, providing greater benefits [21,22]. Furthermore, it has been reported that the planting of trees in wind corridors is associated with a significantly higher cooling in downwind areas compared to leeward ones [20]. Increasing grassy areas is conditionally found to present a suitable intervention to improve pedestrians' thermal comfort [23,24]. Moreover, a combination of GI is particularly effective due to potentially synergistic cooling impacts [25], e.g., combinations of tree-based and grassy GI elements, or a combined implementation of surface vegetation and green roofs or green facades [25–29]. Although the latter may provide limited benefits to outdoor thermal conditions, they may pose alternatives, particularly in dense urban settings with limited ground (planting) space [30].

However, there are certain challenges that remain for a more effective adoption of GI for heat mitigation. These challenges include gaps in linking factors that mediate cooling benefits, e.g., regarding type, design, composition, and density of GI within built-up structures, to inform practitioners more explicitly on relationships between GI configuration and urban morphology. Uncertainties also remain in the contribution of building-related greenery such as green walls and green roofs to cooling and improving OTC at the pedestrian level, and with respect to synergistic, cumulative cooling impacts of heterogeneous GI [5,6,31]. With regard to the presented case study, it is emphasized that such knowledge gaps concern particularly (Southeast) Asian (developing) countries and cities, perhaps apart from China [6,16], and they seem to be particularly pronounced in the case of Vietnam,

where only a few specific case studies could be identified. For a business district quarter in Ho Chi Minh City, an assessment of the (combined) impacts of building orientation, surface materials, and greening on air temperature and OTC concluded that street greenery, i.e., a maximization of street tree plantings, is associated with the most noticeable cooling impact and improvement of OTC, derived from physiological equivalent temperature (PET) [32]. Furthermore, also focusing on Ho Chi Minh City, thermal comfort around so-called "shop-house" dwellings has been assessed to compare air temperature across different urban morphologies [33], and in the city of Ha Tinh, PET was modeled for a residential block, concluding that in comparison to larger areas of grassy vegetation, tree canopies are more suitable for the improvement of OTC, and that waterbodies effectively cool air, but lead to a potential deterioration of OTC [34].

Against this background, this case study seeks to advance the state of the art by adding to the body of knowledge specific to Southeast Asia and Vietnam, as it is in this region where urban environments tend to suffer particularly from heat today, as microclimatic conditions are dominated by high air temperatures, high humidity, and low wind speeds [35]. It is also here that an anticipated exacerbation of heat stress by climate change urgently calls for effective adaptation and mitigation action. However, evidence for the effectiveness of GI under local conditions is needed to support such measures.

The present paper seeks to address this gap. To do so, this paper suggests the modeling of (simultaneous) greening interventions for the city of Huế, Central Vietnam, along a qualitative and quantitative dimension. Here, quality refers to the choice and heterogeneity of GI. In this regard, first, street trees are proposed as a GI type demonstrated to improve OTC. Second, a focus is on decidedly small greening interventions, i.e., green verges as small, grassy open surfaces within the streetscape. This is in contrast to the state of the art, which typically evaluates the effectiveness of larger treed and open urban green spaces [36–39]. Third, green facades are considered in order to assess their potential under local conditions to deliver pedestrian-level cooling and to contribute to the regulation of OTC. The quantitative dimension refers to the total area and thus the density of modeled greening interventions. It contrasts high-density scenarios that seek a maximization of greening with lower-density interventions that may be less effective overall, however, possibly representing more feasible, practical choices for stakeholders. Consequently, both conceptualized dimensions reflect on benefit-mediating factors related to GI configuration and structure, and the embedding of GI within the urban matrix. Modeling is conducted using ENVI-met 5.0.3 [40], a three-dimensional microscale computational fluid dynamics model commonly used for the assessment of microclimatic conditions at fine resolutions [26,41,42], including the Southeast Asian (SEA) region [43].

Through this approach, this paper seeks to investigate potential (synergistic) cooling impacts on air temperature and OTC, thereby contributing to the state of the art and adding to the body of knowledge in several ways. First, the effectiveness of different GI types for heat adaptation under humid tropical climatic conditions is evaluated individually along the proposed qualitative and quantitative dimension, using the city of Huế, Vietnam, as the case study. Second, with a focus also on decidedly small GI elements such as green verges, the benefits of OTC regulation of potentially underexplored GI types are evaluated, considering that such a small GI may likely pose fewer barriers to their implementation. Third, to identify the synergistic benefits of GI for OTC, impacts of a simultaneous implementation of different types of GI are modeled. Findings can inform local decision makers on GI effectiveness for heat mitigation, here within the context of urban expansion, and thus support mainstreaming of GI in urban planning, thereby contributing to the promotion of human health and well-being, and to the increase of urban resilience, sustainability, and social cohesion [18].

The remainder of the manuscript is organized as follows. First, in the Materials and Methods section, the case study area is outlined. Second, the developed scenarios are introduced, and their implementation and simulation in ENVI-met are described in more detail. Third, the methods used for assessing cooling potential and potential impacts

on OTC based on simulated data are described. The findings from the simulation are subsequently presented in the Results section. Here, the first focus is on the domain, i.e., case study area level. Second, impacts are assessed more specifically at selected times of day. The findings are subsequently discussed, and the paper closes with conclusions drawn.

2. Materials and Methods

2.1. Case Study Area

The city of Huế is located in the Thừa Thiên Huế Province in North-Central Vietnam [44,45]. The city features a tropical monsoon climate [46]. Around 491,000 people live in Huế in an administrative area of around 266 km^2, with a population density of around 1845 people/km^2 [47,48]. Despite higher per capita green space than other major Vietnamese cities, Huế does not meet the standards set by Vietnamese regulations, necessitating local policies to increase green space proportions [49,50]. This challenge is compounded by ongoing urban growth, resulting in the necessity for urban governance to address both the planning and development of housing and the simultaneous provision of urban green spaces.

One such newly developed residential area is An Cuu City, which inspired the case study. The An Cuu City neighborhood consists of several multi-story buildings, three high-rise buildings, community buildings, and a large urban green space with various recreational facilities in the neighborhood's center [51]. The case study area is located in the south-eastern part of An Cuu City (Figure 1), with a total size of 2.53 ha. The investigated area is assumed to be two mirrored blocks of residential or mixed-use built-up, adjacent to and separated by a particularly wide collector road, oriented roughly south-west to north-east (Figure 2, bottom right). Each block comprises a total of six buildings, arranged in two tight rows of three buildings each, parallel to the central main road. The buildings have a height of approximately 20 m and feature small, elongated courtyards separating each row. The buildings are further separated by asphalted parking lots, oriented perpendicular to the main road. Baseline conditions in the study area correspond to limited greenery, particularly grassy surfaces, which include courtyards and a green median on the central collector road (Figure 2). The proposed scenarios expand on this baseline by selectively proposing the implementation of additional GI.

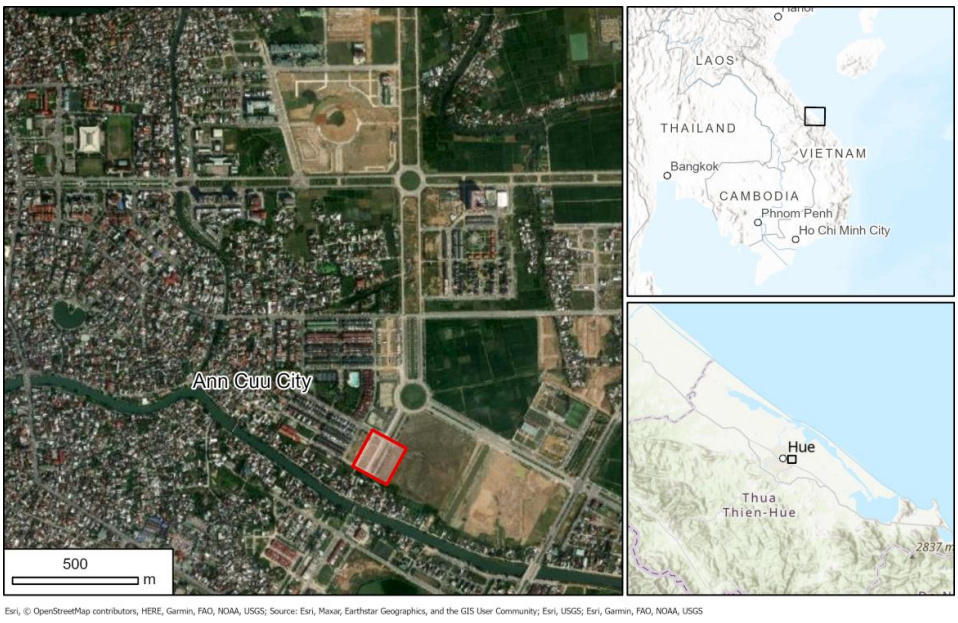

Figure 1. Location of Huế city in Central Vietnam, location of An Cuu City within the city of Huế, and extent of the case study area in the southeastern part of An Cuu City. Squares indicate the location of Huế city in Vietnam, and of the case study area within Huế city.

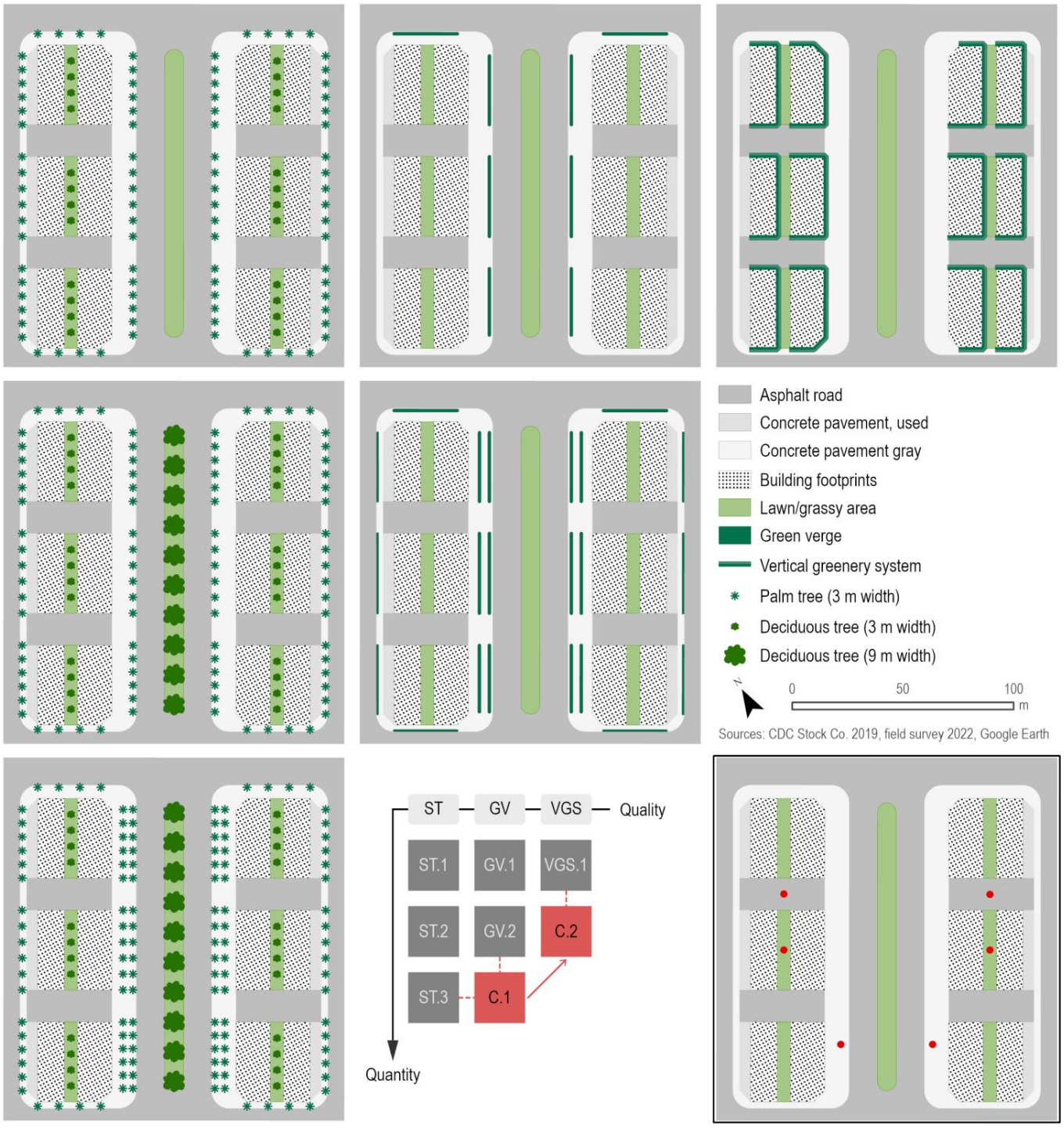

Figure 2. Suggested greening interventions along a qualitative and quantitative dimension. Columns represent the qualitative dimension through choice of GI element, i.e., street trees (ST; **left**), green verges (GV; **middle**), and vertical greenery systems (VGS; **right**). Rows represent the quantitative dimension, i.e., for street trees and green verges, the tree density or green verge area is increased from top to bottom, denoted as ST.1 to ST.3, and GV.1 to GV.2, respectively. Thereby, a so-called triangle of interventions is formed (bottom middle). This intervention triangle is subsequently amended with scenarios C.1 and C.2, which suggest simultaneous greening interventions for a potential maximization of cooling benefits. Scenario C.1 is obtained by combining ST.3 and GV.2, and Scenario C.2 is obtained by combining C.1 and VGS.1. The baseline scenario, including six chosen observer locations, is depicted in the bottom-right corner. See Table 1 for more details on each scenario.

The case study area was selected because it is considered exemplary for local urban development in the context of Huế's urban expansion, with comparatively low but dense multi-story built-up leading to comparatively wide, shallow street canyons. Furthermore, inclusion of the central main road as a key feature of the case study area aims to account for planned expansion of transport infrastructure, thereby addressing associated thermal challenges, but also capitalizing on the opportunities for greening interventions alongside such wider roads.

2.2. Scenario Development

To uncover the potential impacts of greening interventions at the pedestrian level, this paper suggests modeling selected greening interventions. These interventions are described by a set of eight scenarios, forming a so-called intervention triangle (Figure 2). The scenarios are so developed that the suggested qualitative and quantitative dimensions are expressed by them.

First, to uncover the impacts of distinct types of GI individually, the scenarios propose the following GI elements along the qualitative dimension: (i) street trees (STs); (ii) green verges and/or green margins (GVs); and (iii) green facades as a vertical greenery system (VGS). This choice of GI elements for the different scenarios is guided by their likely effectiveness, i.e., their potential to support the regulation of air temperature and improvement of OTC. In the case of STs, the delivery of these benefits is well recognized [16–20]. In the case of GVs, desired impacts are conditionally reported typically for larger grassy surfaces [23,24]. Here, in contrast to such larger open green areas, the focus is on the impact of decidedly smaller roadside vegetation, e.g., to uncover their potential for the retrofitting of streets with limited available space. Similarly, a VGS may capitalize on surfaces otherwise unused; therefore, light shall be shed on the benefits provided by VGSs for the pedestrian level [52,53]. Moreover, the choice and design of GI are also motivated by a reflection of local, technical, and experiential stakeholder knowledge, e.g., regarding the perceived feasibility for local GI implementation [54]. However, in order to also simulate locally accepted interventions that meet stakeholders' preferences, i.e., considering local cultural context, the perceived popularity of GI was also taken into account [54].

Second, regarding the quantitative dimension, scenarios are classified by their total amount and thus the density of greening interventions, thereby reflecting on mediating factors as follows. In scenario ST, factors include the number of trees, which generally increases from scenario ST.1 to ST.3, as well as choice of tree species and planting arrangement; in scenario GV, this includes the number (and thus total area) of green verges, which increases from GV.1 to GV.2, as well as their spatial configuration. In contrast, for a VGS, only a single scenario VGS.1 is formulated (cf. Table 1 and Figure 2).

Third, based on evidence of the potentially increased benefits of simultaneous greening interventions [25–29] compared to the implementation of individual GI types, two further scenarios, C.1 and C.2, are proposed (Figure 2), which model a combination of different types of GI. Thereby, possible cumulative cooling benefits due to synergies in the impacts of diverse greening interventions shall be captured. The GI types considered in these scenarios follow both the conceptualized qualitative and quantitative dimension. Regarding the former dimension, previously individually modeled GI types are combined iteratively, and for the latter dimension, potential synergistic impacts are maximized. Therefore, in scenario C.1, scenario ST.3 is combined with GV.2, and in scenario C.2, the density of GI is further increased by combining scenario C.1 with VGS.1.

Table 1. Description of proposed scenarios. For visualization of scenarios, please refer to Figure 1.

Scenario	Description
Baseline	The amount of greenery under baseline conditions is comparatively sparse, including courtyard greening by lawns, as well as a grassy central median on the central main road. Both the green courtyards and the grassy median strip are about 0.13 ha in size, with the total green area reaching about 0.27 ha.
ST.1	Like baseline, with 24 small deciduous trees proposed in the six courtyards, and 88 palm trees considered in tree pits along the block perimeters. With a total of 112 trees, the tree density reaches about 44 trees per ha in this scenario, and the total green area is equal to 0.27 ha.
ST.2	Like ST.1, with an additional 10 large deciduous trees added in the main road's grassy median. In this scenario, the total tree count increases to 122, with a tree density of 48 trees per ha, and the total green area is 0.27 ha.
ST.3	Like ST.2, with an additional 36 palm trees, to form double rows of palm trees along either side of the central main road. The total tree count is 158, and the tree density 62 trees per ha, and the total green area is 0.27 ha.
GV.1	Like baseline, with additional green verges. The GV.1 scenario prioritizes green verges on wider sidewalks, i.e., on the northern block edges, as well as along either side of the central main road. In total, green verges increase the green area by 0.05 ha, so that the total green area in GV.1 is about 0.32 ha.
GV.2	Like GV.1, with added green verges along outer roads, and a second row of green verges parallel to the central main road. The additional green verges are equal to 0.1 ha in size, increasing the total green area in this scenario to 0.42 ha.
VGS.1	Like baseline, but with added green facades on the northern, eastern, and southern building faces, up to a height of 6 m from ground level. The ground-based green area remains at 0.27 ha.
C.1	This scenario seeks to identify combined and added impacts of ST.3 and GV.2.
C.2	This scenario seeks to identify combined and added impacts of ST.3, GV.2, and VGS.1.

2.3. Model Implementation and Validation

The presented scenarios were subsequently implemented in GIS, translated into ENVI-met, and simulated. Scenario implementation in GIS was conducted in ArcGIS Pro 3.0.1. [55]. Baseline conditions were adapted from digitized planning documents and a visual inspection of Google Earth Imagery, which has been augmented with ground truth information from field observations. Subsequently, the greening interventions suggested in the proposed scenarios were digitized. The translation of scenarios from GIS to ENVI-met was subsequently conducted using ENVI-met Monde. This translation is supported by a compilation of surface materials and building materials relevant to the case study area, with the respective default materials used from the ENVI-met library indicated in Table 2. Moreover, vegetation elements provided by ENVI-met, i.e., palm trees and small as well as large deciduous trees, were used across scenarios (Table 1 and Figure 2); however, they were adapted as needed to represent local vegetation characteristics. Here, for palm trees, default ENVI-met palm trees were re-used. For deciduous trees, default deciduous trees were adapted to the tropical conditions of the case study area, i.e., with their profile changed to represent evergreen trees (Table 2). For the proposed green verges, default ENVI-met grass material was used (Table 2), but with an adapted grass height of 25 cm. For all other grassy surfaces, default ENVI-met grass with a height of 15 cm was used. The implementation of the VGS mimicked modular green walls, i.e., modules with a substrate depth of 15 cm and a plant thickness of 35 cm, atop the concrete wall up to a height of 6 m. This type of VGS is expected to have the greatest impact on microclimatic conditions compared to other types of VGS [56,57]. VGS modules are utilized on the northern, eastern, and southern building faces to provide the highest thermal performance of VGSs [30,56]. Scenarios were run with ENVI-met 5.0.3 using model parameters, as shown in Table 2.

For model calibration and validation, a field measurement campaign was conducted on the premises of the Mientrung Institute for Scientific Research (MISR). The MISR premises were modeled in Rhino 7 [58] and later translated into ENVI-met using Grasshopper's

Dragonfly Legacy plugin [59,60]. Using HOBO MX23021 Bluetooth loggers, air temperature (T_a) and relative humidity (RH) were measured at a height of 1.5 m at three selected measurement points in five-minute intervals over a period of four consecutive days, starting at 10 a.m. on 5 November 2021 and ending at 10 a.m. on 9 November 2021. A period of 48 h was then simulated, starting on 5 November 2021, using simple forcing for meteorological boundary conditions; hence, hourly weather data from the Huế weather station were used for this simulation. Simulated data for 6 November 2021 were subsequently compared with measured data, and the coefficients of determination (R^2) were calculated, with R^2 ranging from 0.7989 to 0.8625 for T_a and from 0.7900 to 0.8780 for RH, respectively. These R^2 values indicate a good model fit for the study region, as reported in previous studies on tropical and subtropical areas [61–64]. The associated root mean square error (RMSE) ranges from 1.2387 °C to 2.8641 °C for T_a and from 6.7387% to 8.1599% for RH, mean absolute error (MAE) from 1.0824 °C to 2.004 °C for T_a and from 5.5131% to 7.4952% for RH, and mean bias error (MBE) from 0.639 °C to 1.541 °C for T_a and from 4.265% to 7.495% for RH.

Table 2. Input parameters for the initialization of the ENVI-met simulation.

Parameter	Setting
Location	Huế, Thừa Thiên Huế Province, Vietnam
Start of simulation	19 April 2019, 12:00 a.m./midnight
Duration [h]	24
Model grid size (x, y, z)	77 × 82 × 15
Resolution (dx, dy, dz) [m]	2 × 2 × 2
Telescoping factor [%]	30
Telescoping starting height [m]	20
Model rotation [°]	28.60
Building material	Roofing: Tile [0100R1]; Walls: Plastered concrete wall consisting of Default Plaster [0100PL] (1 cm); Concrete: Hollow block [0000C3] (30 cm); Default Plaster [0100PL] (1 cm)
Surface material	Main road, parking lots: Asphalt Road [0100ST]; Sidewalks: Concrete Pavement Gray [0100PG]; Sealed surfaces: Pavement (Concrete), used/dirty; Unsealed surfaces: Default Unsealed Soil (Sandy Loam) [010000]
Vegetation	Palm tree: Crown diameter (width) 3 m, height 5 m, medium trunk, LAD [1] of 0.60, tropical (evergreen) profile; Small deciduous tree: Crown diameter (width) 3 m, height 5 m, medium trunk, LAD of 1.10, spherical crown shape, tropical (evergreen) profile; Large deciduous tree: Crown diameter (width) 9 m, height 15 m, large trunk, LAD of 1.10, cylindric crown shape, tropical (evergreen) profile; Grass: Axonopus compressus, LAD of 0.30, tropical (evergreen) profile
Meteorological boundary conditions	Simple forcing
Air temperature (min/max) [°C]	26.4/39.4
Relative humidity (min/max) [%]	45/96
Wind speed [m s^{-1}]	2.00
Wind direction [°]	67.50
Cloud cover (low/medium/high) [okta]	0/0/4
Raytracing precision	Finer resolution
Height segment angles resolution [°]	15
Azimuthal segment angles resolution [°]	15

[1] Leaf area density.

2.4. Assessment of Cooling and Outdoor Thermal Comfort

The impacts of ENVI-met-simulated scenarios were evaluated using the *scipy* package for the Python programming language [65]. Here, the focus is on the parameters air tem-

perature (T_a), relative humidity (RH), mean radiant temperature (T_{mrt}), and the Universal Thermal Climate Index (UTCI). T_a is used for a direct assessment of cooling potential. RH and T_{mrt} are assessed as drivers of thermal discomfort [66,67], and against the background of greening interventions, increasing RH due to promoting evapotranspiration, thus giving rise to potentially adverse feedback loops, but limiting T_{mrt} due to the interception of solar radiation [68,69]. UTCI was chosen as an indicator of OTC, which was determined for all simulated scenarios using Biomet 5.0.3 [40]. UTCI is based on a multi-node model of thermoregulation that considers air temperature, relative humidity, solar radiation, and wind speed [70–72]. UTCI is considered a universal index that is applicable across climates, seasons, and spatial scales [73] and that shows strong correlations to other thermal indices, including Standard Equivalent Temperature (SET), PET, or wet-bulb globe temperature [12,72,74]. UTCI is chosen in favor of PET due to its independence of a person's characteristics such as age or gender [71].

Impacts of GI on T_a, RH, T_{mrt}, and UTCI are assessed at a height of 1.4 m above ground level. This height is seen as representative for the pedestrian level considering local context, as it should roughly approximate an average pedestrian's chin-to-shoulder height. In this regard, first, differences in either parameter compared to baseline are evaluated over time of day, i.e., hourly from 6 a.m. to 6 p.m., averaged at the domain level. Thereby, overall impacts on the chosen parameters mediated by the factors GI choice, GI heterogeneity, and GI density, as proposed through the qualitative and quantitative dimensions, shall be uncovered at the case study level. Second, for selected times of day, i.e., morning (6 a.m.), noon (12 p.m.), afternoon (3 p.m.), and evening (6 p.m.), heat stress is determined based on UTCI [71], and changes in T_a, RH, T_{mrt}, and UTCI are evaluated accordingly in a spatially explicit manner, i.e., on a per-pixel basis, to identify local cooling impacts and potential improvements of OTC tied to individual GI elements more closely. Here, to support the interpretation of the findings, a simple classification of differences in UTCI is suggested. In addition, six observer locations within the pedestrian space are evaluated, which are situated in different settings of the wider pedestrian space, i.e., parking lots, courtyards, and sidewalks of the wide main road. The observers follow the prevailing wind direction and are thus mirrored between the downwind and the leeward block structures (Figure 2).

The Wilcoxon signed-rank test [75], a non-parametric test of location for paired data, was used to detect the statistical significance of differences between proposed interventions and baseline [76].

3. Results

Simulated T_a, RH, T_{mrt}, and UTCI under baseline conditions provide the reference frames for assessing the potentials and effectiveness of proposed greening interventions in regulating T_a and UTCI, and thus OTC. As mentioned, this effectiveness is evaluated, first, averaged at the level of the domain, i.e., the case study area, and second, spatially explicitly on a per-pixel basis, supported by selected observer locations.

With respect to domain-level baseline conditions, in line with local climatic conditions, there are considerable changes in temperatures, with T_a, T_{mrt}, and UTCI generally following similar patterns over the daytime, but with changes in T_{mrt} and UTCI being more pronounced. Until noon, T_a increases sharply, from 27.2 ± 0.3 °C (6 a.m.) to 38.9 ± 0.8 °C (12 p.m.). In the afternoon hours, T_a starts to decrease slowly to 37.8 ± 0.5 °C (3 p.m.) and 34.0 ± 0.2 °C (6 p.m.), respectively (Figure 3a). RH is high in the morning hours at 87.0 ± 4.3% (6 a.m.), then decreases to about 43.5 ± 1.2% at 12 p.m., in line with rising temperatures. Subsequently, from noon to evening, RH starts to increase again, reaching 49.3 ± 2.0% at 3 p.m., and 56.9 ± 2.2% at 6 p.m. (Figure 3b). In contrast to T_a, mirroring the sun's elevation, T_{mrt} rises sharply to 60.2 ± 4.1 °C until noon, remains high at 53.1 ± 8.4 °C at 3 p.m., and then decreases sharply to 27.2 ± 0.7 °C at 6 p.m. (Figure 3c). The range of the modelled T_{mrt}, and thus variance, is significantly higher than for T_a. UTCI follows a pattern similar to T_{mrt}, but with a lower amplitude, i.e., reaching 45.5 ± 1.3 °C at noon. Until 3 p.m., UTCI decreases to 43.2 ± 2.0 °C, and further to 34.0 ± 0.4 °C at 6 p.m. (Figure 3d). On average, UTCI indicates

strong (UTCI > 32 °C) to very strong (UTCI > 38 °C) heat stress during most hours of day. Similar to T_{mrt}, the variance of UTCI is high. Due to this, extreme heat stress (UTCI > 46 °C) may also be observed at selected locations within the case study area.

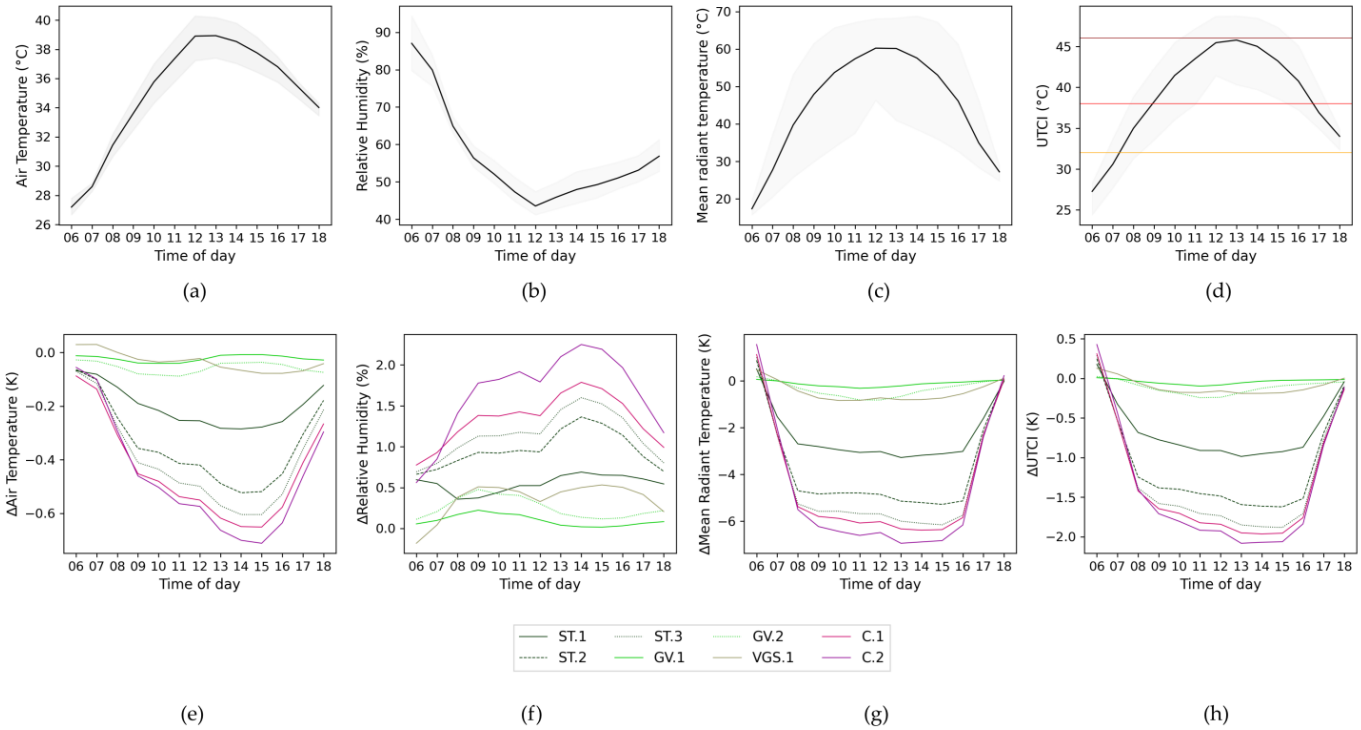

Figure 3. Simulated impacts averaged at the domain level, at a height of 1.4 m above ground level: (**a**) mean and range of air temperature (T_a, °C) under baseline; (**b**) mean and range of relative humidity (RH, %) under baseline; (**c**) mean and range of mean radiant temperature (T_{mrt}, °C) under baseline; (**d**) mean and range of UTCI (°C) under baseline. Plotted thresholds indicate strong (UTCI > 32 °C), very strong (UTCI > 38 °C), and extreme heat stress (UTCI > 46 °C) [71]; (**e**) cooling potential over time of day, in terms of averaged differences in modeled T_a to baseline (K), per scenario; (**f**) averaged differences in modeled RH to baseline (%), per scenario; (**g**) averaged differences in modelled T_{mrt} to baseline (K), per scenario; (**h**) averaged differences in modeled UTCI to baseline (K), per scenario.

Looking at the average cooling potential, i.e., lowering of T_a in each scenario at the domain level, it becomes clear that with respect to the qualitative dimension, street trees appear to have the highest cooling potential compared to other greening interventions. This remains true for all times of day; however, maximum impacts are realized in these scenarios between noon and afternoon (Figure 3e). With respect to tree density and, thus, the quantitative dimension of the proposed intervention triangle, there are noticeable differences in the cooling delivered between the tree-based scenarios. While averaged cooling is only up to −0.3 K for the low-density scenario ST.1, it is up to −0.5 K (ST.2) and −0.6 K (ST.3) for the higher-density interventions. The average cooling potential of the remaining GI types is limited compared to tree-based interventions. For the GV scenarios, the maximum average cooling is estimated at −0.1 K (GV.2), with maximum impacts predicted during morning hours. The modeled average cooling potential of green walls realized in scenario VGS.1 appears to be yet more varied, with potentially detrimental impacts predicted in the morning, and cooling of up to −0.1 K during afternoon hours. Finally, regarding potentially synergistic benefits provided by heterogeneous GI implementation, it is found that in the corresponding scenarios C.1 and C.2, such synergistic effects may become evident, with average cooling potentials of up to −0.7 K exceeding the modeled impacts of individual greening interventions.

The simulated changes to RH remain comparatively modest (Figure 3f). Apparently, a higher density of greening, i.e., a higher number of trees or larger total green area, seems to be associated with higher increases in RH; for scenarios ST, average RH increases by about +0.7% (ST.1) to +1.6% (ST.3), and for scenarios C.1 and C.2, by up to +1.8% and +2.3%, respectively. In contrast, changes to RH in scenarios GV and VGS.1 are small, with up to +0.5% (VGS.1).

With respect to T_{mrt}, it is found that during daytime margin hours, tree-based interventions seemingly lead to an increase of T_{mrt} at the domain level, with up to +1.0 K (ST.3) and +1.6 K (C.2), respectively (Figure 3g). For the lower-density tree-based intervention ST.1, T_{mrt} increases by about +0.5 K at these times of day; for VGS.1, the impact on T_{mrt} is similar in magnitude. With an increase in T_{mrt} of up to +0.2 K (GV.2) at the domain level, the least adverse impacts on T_{mrt} are estimated for GV scenarios. Conversely, from about 9 a.m. to 3 p.m., tree-based and combined interventions in particular seemingly decrease T_{mrt} considerably at the domain level, by up to −3.3 K (ST.1), −6.2 K (ST.3), and −6.9 K (C.2), respectively. In contrast, the impact on T_{mrt} at the domain level in GV and VGS scenarios is limited at these times, with about −0.8 K for both GV.2 and VGS.1.

Regarding OTC, due to their comparatively high cooling potential with respect to T_a and regulation of T_{mrt}, tree-based (and, therefore, combined) interventions may intuitively be considered as those interventions that provide effective regulation of OTC. Indeed, looking at changes in UTCI (Figure 3h), the averaged impact on UTCI seems highest in the associated scenarios ST.1, ST.2, ST.3, C.1, and C.2; in the tree-based interventions, UTCI is lowered on average by −1.0 K (ST.1), −1.6 K (ST.2), and −1.9 K (ST.3), and in combined interventions by −2.0 K (C.1) and −2.1 K (C.2). It also needs to be noted that, as before, potentially undesired impacts on UTCI become apparent. This particularly applies to tree-based interventions, which potentially increase UTCI by up to +0.3 K (ST.3) and +0.4 K (C.2) during daytime margin hours.

In this regard, it appears that compared with the abovementioned T_a cooling potential, relatively small changes in T_a may translate to more pronounced changes in UTCI. This seems particularly true for the GV and VGS scenarios. For example, despite their apparently negligible impact on T_a, their impact on UTCI is more pronounced, as these small GI types may regulate UTCI at the domain level by up to −0.2 K (GV.2 and VGS.1; cf. Figure 3h). Therefore, for the improvement of OTC, not only T_a cooling but particularly the regulation of radiant load seems to be an important determinant. Moreover, in contrast to the impacts of interventions on the chosen parameter at the domain level, i.e., averaged for the case study area, it needs to be noted that local impacts of greening interventions may be substantially higher. Therefore, for a closer inspection of local impacts, changes in T_a, RH, T_{mrt}, and UTCI are subsequently mapped and assessed for morning (6 a.m.), noon (12 p.m.), afternoon (3 p.m.), and evening (6 p.m.).

3.1. Morning Conditions

At 6 a.m., mostly moderate heat stress is estimated under baseline conditions. Cooling potential is low across all scenarios, although statistically significant for T_a ($p < 0.001$; H_A: $T_{a,scenario} < T_{a,baseline}$) except for VGS.1 (Figure 4). Nominally, tree-based interventions, including combined scenarios, achieve the highest cooling impacts. For example, for ST.3, the local cooling is up to −0.5 K (Table 3). However, when consulting UTCI, and in line with findings at the domain level, the predicted cooling potential seemingly does not translate into improvements of OTC. Instead, increasing UTCI with potentially detrimental impacts on OTC is estimated. While this may have been anticipated for VGS.1, for which an increase in T_a was modeled at this time of day ($p < 0.001$; H_A: $T_{a,VGS1} > T_{a,baseline}$), it must be noted that the remaining scenarios seemingly do not result in a substantial regulation of UTCI, or may similarly be associated with adverse impacts. The latter particularly applies to all tree-based and thus combined interventions, with changes in UTCI at the domain level estimated from +0.2 K (ST.3) to +0.4 K (C.2), and with changes in UTCI of up to +1.5 K locally ($p < 0.001$; H_A: $UTCI_{ST\cdot X} > UTCI_{Baseline}$). Potential causes for these adverse impacts may be, on the one

hand, an increase in RH, which, at +4.6% (C.1), is the highest for tree-based and thus also combined interventions, and, on the other hand, an increase in T_{mrt} by up to +4.5 K (C.2), e.g., due to the trapping of longwave radiation under tree canopies. However, changes in RH with the exception of VGS.1 ($p > 0.05$; H_A: $RH_{Baseline} < RH_{scenario}$) and T_{mrt} ($p > 0.05$; H_A: $T_{mrt,Baseline} < T_{mrt,scenario}$) remain not significant (Figure 4 and Table 3).

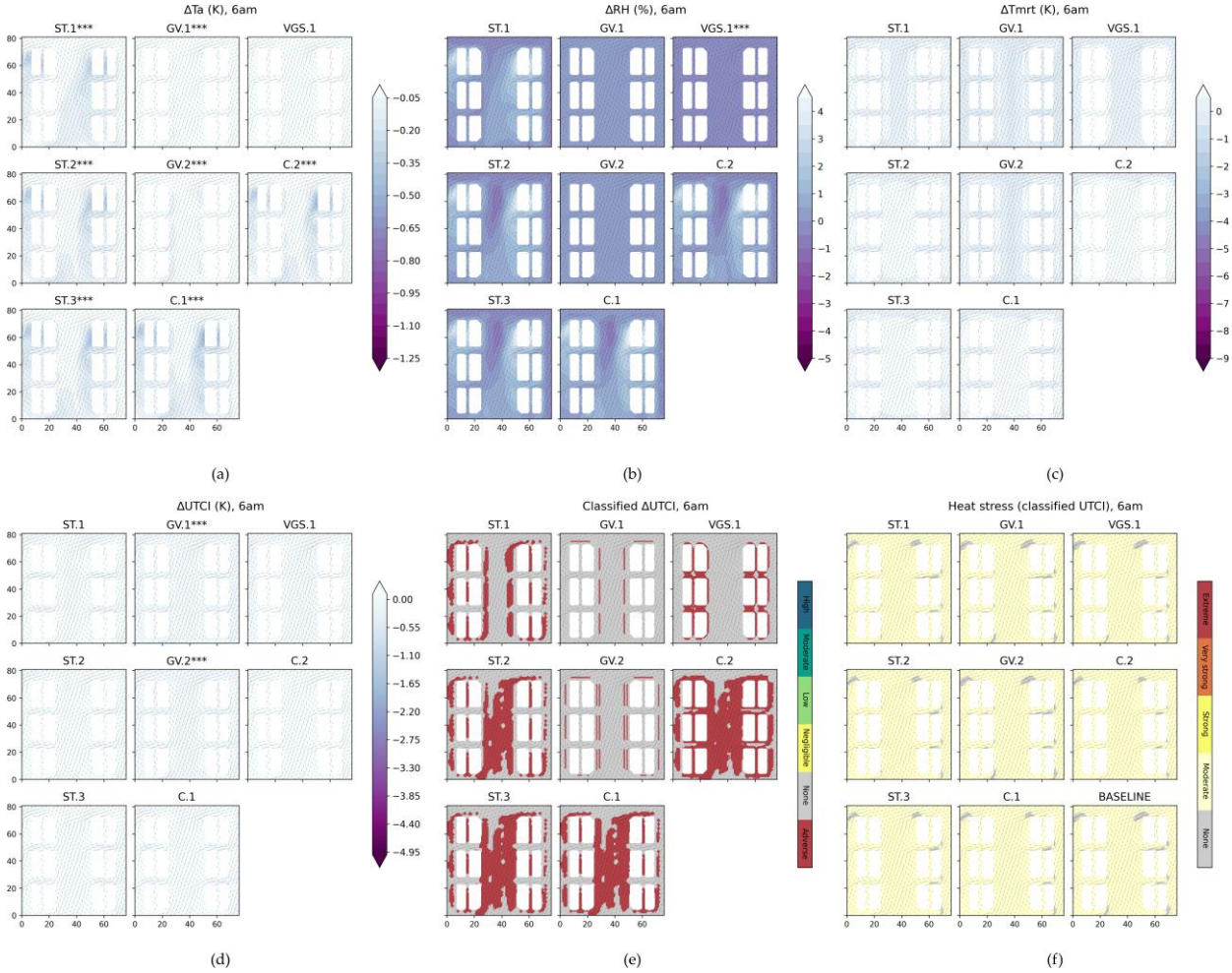

Figure 4. Simulation results at the pedestrian level for 6 a.m.: (**a**) local cooling potential, i.e., modeled difference in air temperature (K) compared to baseline; (**b**) changes in relative humidity (%) compared to baseline; (**c**) difference in T_{mrt} (K) compared to baseline; (**d**) local regulation of OTC, i.e., difference in UTCI (K) compared to baseline; (**e**) classified local regulation of OTC, where Adverse: $\Delta UTCI > +0.25$; None: $-0.25 < \Delta UTCI \leq +0.25$; Negligible: $-0.5 < \Delta UTCI \leq -0.25$; Low: $-1.0 < \Delta UTCI \leq -0.5$; Moderate: $-2.0 < \Delta UTCI \leq -1.0$; High: $-2.0 > \Delta UTCI$; (**f**) heat stress, with classes derived through a classification of modeled UTCI (°C), where None: $UTCI \leq 26$; Moderate: $26 < UTCI \leq 32$; Strong: $32 < UTCI \leq 38$; Very strong: $38 < UTCI \leq 46$; Extreme: $UTCI > 46$ [71]. Prevailing wind speed and wind direction are shown as a Quiver plot. The significance of differences is based on a one-sided Wilcoxon signed-rank test (H_A: scenario < baseline) and is denoted as follows: ***, highly significant ($p < 0.001$); non-significant otherwise ($p > 0.05$).

Table 3. Mean, standard deviation (Std), and range (minimum, maximum) of simulated differences to baseline for the parameters air temperature (T_a), relative humidity (RH), mean radiant temperature (T_{mrt}), and UTCI per scenario (Scen.) at the chosen times of day. Shading of cells emphasizes comparatively high mean, maximum, or minimum differences, indicating beneficial or potentially adverse impacts on T_a, RH, T_{mrt}, and UTCI.

Scen.	ΔT_a (K) [1]				ΔRH (%) [2]				ΔT_{mrt} (K) [1]				ΔUTCI (K) [1]			
	Mean	Std	Min	Max	Mean	Std	Min	Max	Mean	Std	Min	Max	Mean	Std	Min	Max
6 a.m.																
ST.1	−0.07	0.07	−0.39	0.06	0.60	0.67	−0.39	3.42	0.52	0.55	−0.15	2.94	0.18	0.20	−0.26	1.06
ST.2	−0.06	0.09	−0.40	0.11	0.66	0.78	−0.90	3.85	0.88	0.72	−0.07	3.23	0.25	0.21	−0.18	1.11
ST.3	−0.07	0.09	−0.47	0.11	0.69	0.80	−0.86	4.36	1.01	0.81	−0.08	3.57	0.29	0.24	−0.17	1.32
GV.1	−0.01	0.01	−0.07	0.00	0.06	0.05	0.01	0.38	0.07	0.23	−0.01	1.49	0.01	0.06	−0.02	0.39
GV.2	−0.03	0.02	−0.11	−0.01	0.11	0.08	0.01	0.61	0.18	0.37	−0.02	1.57	0.03	0.09	−0.05	0.41
VGS.1	0.03	0.02	0.01	0.08	−0.18	0.14	−0.81	−0.03	0.47	0.59	0.01	2.63	0.13	0.14	0.01	0.67
C.1	−0.09	0.09	−0.50	0.10	0.78	0.81	−0.82	4.59	1.13	0.96	−0.08	4.02	0.31	0.28	−0.20	1.47
C.2	−0.06	0.08	−0.49	0.11	0.56	0.73	−0.86	4.45	1.56	1.01	−0.01	4.48	0.43	0.31	−0.07	1.50
12 p.m.																
ST.1	−0.26	0.11	−0.65	0.05	0.52	0.28	−0.02	1.44	−3.02	3.12	−15.1	−0.33	−0.91	0.76	−4.07	−0.23
ST.2	−0.42	0.21	−1.03	0.07	0.94	0.58	−0.06	2.61	−4.85	4.07	−18.2	−0.66	−1.49	1.04	−5.02	−0.30
ST.3	−0.50	0.24	−1.27	−0.09	1.16	0.71	0.05	3.67	−5.68	4.56	−18.7	−0.69	−1.74	1.16	−5.15	−0.37
GV.1	−0.03	0.02	−0.14	0.00	0.11	0.10	−0.01	0.69	−0.28	0.78	−5.91	0.14	−0.08	0.19	−1.53	0.04
GV.2	−0.07	0.03	−0.21	−0.03	0.30	0.17	0.10	1.00	−0.81	1.40	−6.62	−0.01	−0.24	0.35	−1.73	−0.03
VGS.1	−0.02	0.02	−0.10	0.06	0.33	0.30	0.03	1.40	−0.72	0.80	−4.91	−0.01	−0.16	0.17	−1.13	0.04
C.1	−0.55	0.26	−1.46	−0.11	1.38	0.79	0.13	4.50	−6.02	4.85	−19.2	−0.76	−1.84	1.23	−5.23	−0.41
C.2	−0.57	0.26	−1.50	−0.12	1.79	0.93	0.22	5.46	−6.48	4.80	−19.7	−0.80	−1.93	1.22	−5.41	−0.43
3 p.m.																
ST.1	−0.28	0.09	−0.55	−0.03	0.65	0.27	0.15	1.28	−3.11	3.45	−18.2	−0.35	−0.93	0.84	−4.93	−0.14
ST.2	−0.52	0.23	−1.17	−0.05	1.29	0.69	0.23	3.01	−5.28	4.99	−18.5	−0.63	−1.62	1.23	−5.20	−0.37
ST.3	−0.60	0.26	−1.22	−0.20	1.52	0.81	0.34	3.47	−6.15	5.65	−21.1	−0.66	−1.88	1.39	−5.47	−0.42
GV.1	−0.01	0.01	−0.06	0.04	0.02	0.03	−0.10	0.20	−0.08	0.23	−2.33	0.09	−0.02	0.05	−0.57	0.05
GV.2	−0.04	0.02	−0.10	0.02	0.12	0.06	−0.01	0.50	−0.29	0.51	−3.38	0.00	−0.09	0.12	−0.89	0.01
VGS.1	−0.08	0.05	−0.27	−0.02	0.53	0.46	0.05	2.07	−0.73	0.86	−4.84	−0.01	−0.18	0.19	−1.20	0.00
C.1	−0.65	0.26	−1.32	−0.23	1.71	0.85	0.43	4.09	−6.36	5.79	−22.3	−0.71	−1.96	1.42	−5.91	−0.44
C.2	−0.71	0.27	−1.40	−0.26	2.19	0.97	0.47	5.25	−6.83	5.64	−22.5	−0.78	−2.06	1.38	−5.98	−0.51
6 p.m.																
ST.1	−0.12	0.05	−0.39	−0.05	0.54	0.34	0.09	2.47	−0.01	0.32	−1.54	1.71	−0.04	0.12	−0.50	0.51
ST.2	−0.18	0.06	−0.43	−0.07	0.70	0.39	0.08	2.62	0.04	0.46	−1.52	1.71	−0.09	0.13	−0.57	0.47
ST.3	−0.21	0.08	−0.44	−0.08	0.80	0.44	0.13	2.67	0.04	0.49	−1.85	1.82	−0.11	0.14	−0.62	0.49
GV.1	−0.03	0.02	−0.14	−0.01	0.08	0.07	0.01	0.50	0.03	0.16	−0.05	1.10	−0.01	0.03	−0.07	0.21
GV.2	−0.07	0.03	−0.22	−0.03	0.22	0.12	0.06	0.76	0.06	0.23	−0.10	1.16	−0.04	0.05	−0.12	0.18
VGS.1	−0.04	0.04	−0.18	−0.01	0.21	0.19	0.022	0.92	0.12	0.24	−0.54	1.13	0.00	0.05	−0.17	0.22
C.1	−0.27	0.09	−0.54	−0.10	0.99	0.50	0.21	2.90	0.07	0.55	−1.87	2.05	−0.14	0.16	−0.67	0.51
C.2	−0.30	0.11	−0.57	−0.11	1.17	0.61	0.22	3.46	0.23	0.59	−1.86	2.21	−0.11	0.17	−0.65	0.52

[1] Color shade indicates magnitude of impact, with higher impacts visualized by more intensive shade. Decreases in temperature are indicated using blue shading and increases using red shading. [2] Color shade indicates magnitude of impact, with higher impacts visualized by more intensive shade. Decreases in relative humidity are indicated using orange shading and increases using purple shading.

3.2. Noon Conditions

At 12 p.m., heat stress is very strong up to extreme under baseline conditions (Figure 5); however, all interventions appear to provide some level of cooling and, simultaneously, seemingly contribute to the improvement of OTC. However, the magnitude and spatial extent of estimated benefits may vary considerably (Figure 5).

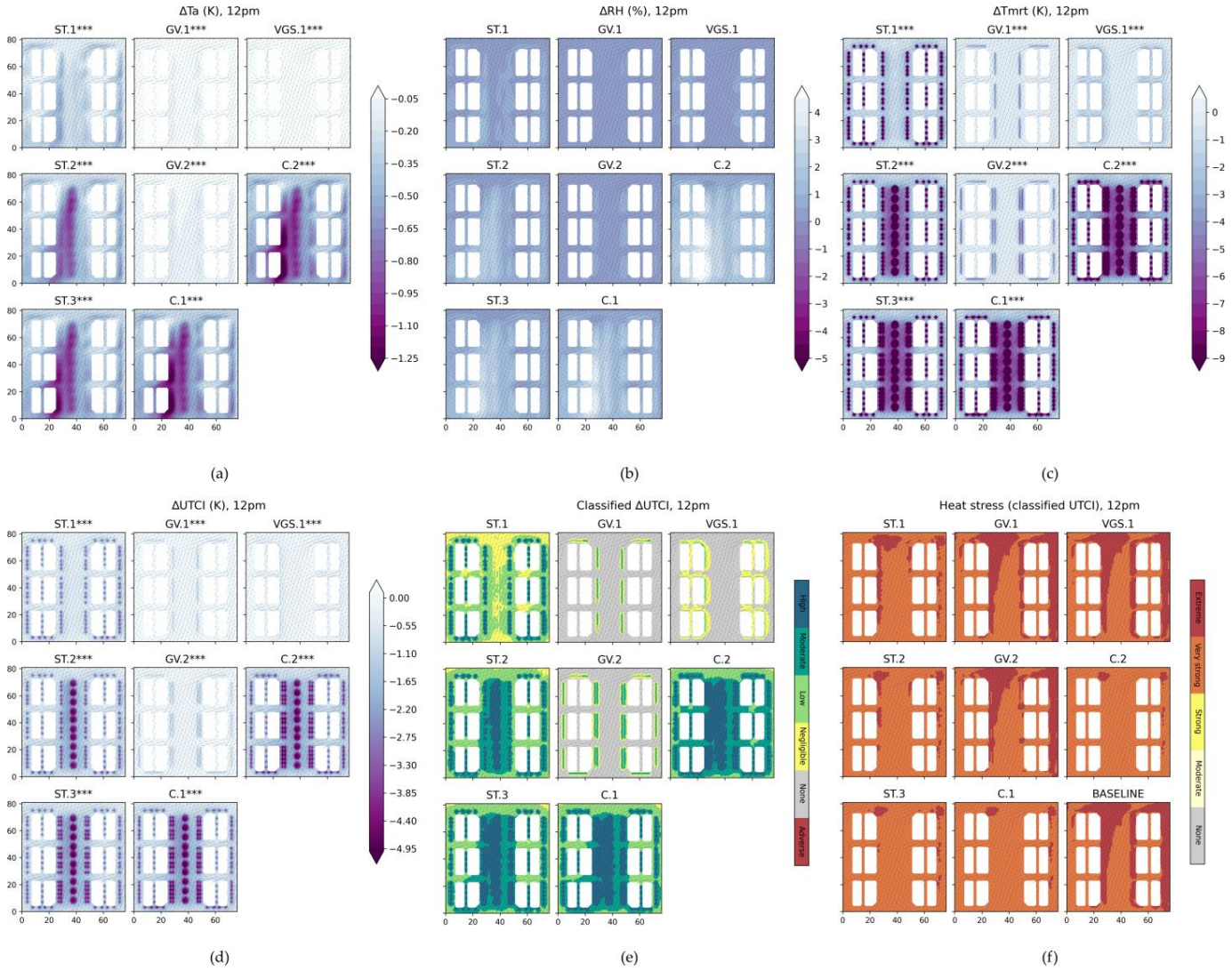

Figure 5. Simulation results at the pedestrian level for 12 p.m.: (**a**) local cooling potential (K); (**b**) changes in relative humidity (%); (**c**) difference in T_{mrt} (K); (**d**) local regulation of OTC; (**e**) classified local regulation of OTC; (**f**) heat stress. Prevailing wind speed and wind direction are shown as a Quiver plot. Please refer to Figure 4 for a description of the classes and significances. ***, highly significant ($p < 0.001$); non-significant otherwise ($p > 0.05$).

Perhaps unsurprisingly, cooling mostly follows the suggested (planting) locations of GI elements, thus closely mirroring sidewalks along block perimeters. However, especially in the higher-density tree-based interventions ST.2 and ST.3, in correspondence to the large deciduous trees proposed along the central road's median, a more pronounced local cool island is formed, spanning considerable portions of the street space, and partially extending into parking lots between buildings. Comparing locally achieved T_a cooling to averaged T_a cooling potential, it was found that local impacts may be considerably higher. For example, for ST.3, the local cooling potential is up to −1.3 K, about 3.4-fold the average (Table 3). Cooling achieved in the GV and VGS scenarios is comparatively small, both on average and locally. However, in GV.2, the maximum local T_a cooling of −0.2 K is again about 3-fold the average, and green facades in VGS.1 deliver cooling of up to −0.1 K locally, about 4.3-fold the average. Spatially, however, these effects are limited to the near proximity of green verges, and to parking lots in front of the north-eastern building faces. Thus, in contrast to street trees, the cooling impacts of green verges and green facades on T_a remain highly local. Furthermore, again in line with the findings at the domain level, with up to

−1.5 K, i.e., about 2.6-fold the average, combined GI implementation in scenarios C.1 and C.2 potentially results in the highest domain-level and locally delivered cooling (Figure 5 and Table 3).

It follows that arguably, impacts on OTC, particularly of GV and VGS, may be limited at best. However, as found for the case study level, comparatively small changes in T_a may translate to more significant changes in UTCI, depending on the simultaneous impacts on RH and T_{mrt}. In the case of GV.2, locally, UTCI is regulated by up to −1.7 K, and for VGS.1, it is still up to −1.1 K. Therefore, despite low differences in T_a, especially the higher-density green verge scenario may nonetheless support the regulation of OTC within the pedestrian space, although to a spatially limited extent. Nevertheless, tree-based interventions remain the most effective, with UTCI regulated locally by approximately −4.1 K (ST.1) to −5.2 K (ST.3; cf. Table 3), despite increases in RH in these scenarios by up to 3.7% (ST.3, cf. Table 3); differences in RH in the GV and VGS scenarios are less pronounced (Table 3), and for all scenarios, differences in RH to baseline remain non-significant ($p > 0.05$; H_A: $RH_{Baseline} < RH_{scenario}$, cf. Figure 5). Although higher-density tree-based scenarios are associated with the formation of a local cool island, thus apparently regulating UTCI more widely across the streetscape and pedestrian space with moderate to high impacts on UTCI, as shown in Figure 5, local maxima are seemingly tied to near tree-planting locations. This emphasizes that larger improvements of OTC may be particularly attributable to tree shade blocking direct solar radiation, which is exemplified by the substantial decrease in T_{mrt} by up to −18.7 K (ST.3) under tree canopies (Figure 5 and Table 3), thus underlining the importance of regulating radiant load for improving OTC.

The combined scenarios C.1 and C.2 provide an even higher regulation of UTCI, of up to −5.2 K and −5.4 K, respectively; i.e., the combined implementation of heterogeneous GI is considered to have added benefits for the regulation of UTCI. The addition of green verges to ST.3 in scenario C.1 may significantly enhance tree-based impacts ($p < 0.001$; H_A: $UTCI_{C\cdot1} < UTCI_{ST\cdot3}$), resulting in an enlarged extent of moderate to high UTCI regulation across sidewalks along the central road, where extreme heat stress is reduced to very strong heat stress. Further adding green facades to C.1 in scenario C.2 may similarly support the regulation of UTCI by enhancing impacts from low to moderate within parking lots between buildings, thereby exceeding local impacts in scenarios ST.3 and C.1, respectively ($p < 0.001$; H_A: $UTCI_{C\cdot2} < UTCI_{C\cdot1}$). Therefore, combining tree planting with additional types of GI is expected to synergistically contribute to the regulation of OTC.

3.3. Afternoon Conditions

At 3 p.m., under baseline conditions, heat stress remains very strong, and extreme on eastern sidewalk locations, in line with the expected position of the sun at this time of day (Figure 6). Cooling potential remains significant across interventions ($p < 0.001$; H_A: $T_{a,scenario} < T_{a,baseline}$). For tree-based interventions, it is found that averaged at the domain level, T_a cooling potential increases slightly from noon to afternoon ($p < 0.001$; H_A: $T_{a,ST\cdot X,12\,pm} < T_{a,ST\cdot X,3\,pm}$), but local cooling potential seemingly does not increase further. Like at noon, the higher-density tree-based interventions ST.2 and ST.3, and similarly, the combined scenarios C.1 and C.2, are associated with the formation of a local cool island. This may support the regulation of OTC through a local mitigation of extreme heat stress, particularly within sidewalks (Figure 6). As before, greening interventions may result in slight increases in RH; however, changes in RH remain non-significant across all interventions ($p > 0.05$; H_A: $RH_{Baseline} < RH_{scenario}$, cf. Table 3 and Figure 6). Similar to noon, the strongest impacts on UTCI are tied to tree shade as cast during this time of day, thereby re-emphasizing the importance of tree shade for limiting solar radiation and thus T_{mrt}. Under tree canopies, T_{mrt} is up to −21.2 K (ST.3) to −22.6 K (C.2) lower than baseline; however, with −3.1 K (ST.1) to −6.8 K (C.2), T_{mrt} is also significantly reduced at the domain level (Table 3). This may contribute to the formation of the simulated local cool island, as estimated across the pedestrian space.

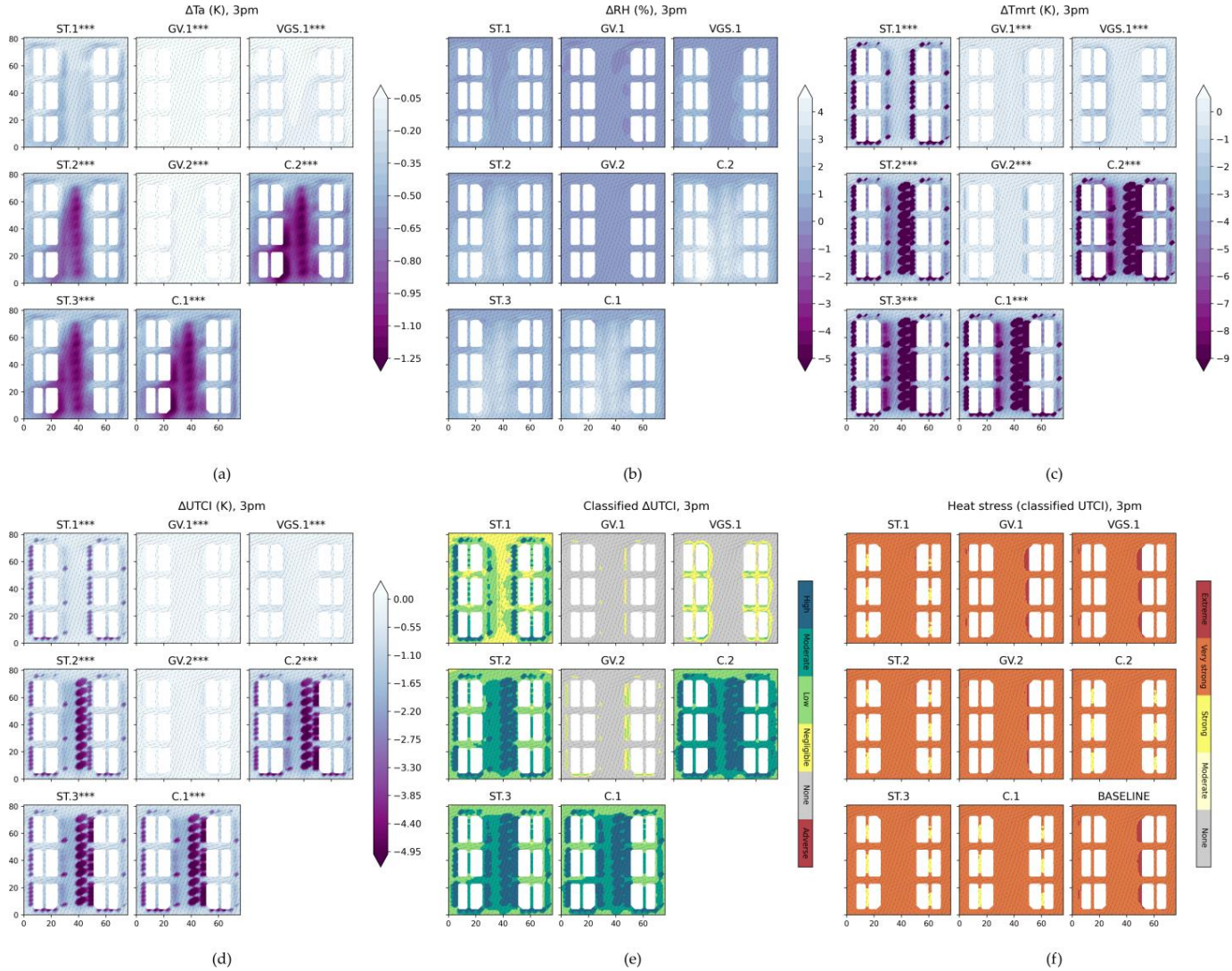

Figure 6. Simulation results at the pedestrian level for 3 p.m.: (**a**) local cooling potential (K); (**b**) changes in relative humidity (%); (**c**) difference in T_{mrt} (K); (**d**) local regulation of OTC; (**e**) classified local regulation of OTC; (**f**) heat stress. Prevailing wind speed and wind direction are shown as a Quiver plot. Please refer to Figure 4 for a description of the classes and significances. ***, highly significant ($p < 0.001$); non-significant otherwise ($p > 0.05$).

In line with findings at the overall case study level, benefits delivered by GV seemingly diminish at this time of day, with maximum local impacts on UTCI of up to −0.9 K being about half the modeled potential at noon (Table 3). Consequently, GV has mostly negligible impacts on OTC at this time of day. However, within parts of the pedestrian space along eastern sidewalk locations, higher-density green verges in GV.2 may support the regulation of OTC to a limited extent. VGSs may provide some local cooling at this time of day, with impacts on UTCI being the highest in parking lots and nearby greened building faces (Figure 6); however, benefits provided appear insufficient to considerably mitigate heat stress in these locations.

3.4. Evening Conditions

At 6 p.m., the modeled heat stress is strong under baseline conditions (Figure 7). Compared to noon or afternoon, T_a cooling potential is lower across all scenarios, although it remains significant ($p < 0.001$; H_A: $T_{a,scenario} < T_{a,baseline}$). Unlike at 12 p.m. or 3 p.m., no extensive local cool island is estimated for higher-density tree-based scenarios at this

time of day; tree-based cooling impacts therefore remain most effective nearby suggested tree planting locations, and thus along the block structure perimeters, achieving maximum impacts on T_a of up to −0.4 K locally (ST.3, cf. Table 3). However, similar to morning conditions, this reduction of T_a seemingly does not effect a substantial improvement in OTC, as UTCI is reduced negligibly, if at all. This may be due to the limited effectiveness of trees to regulate T_{mrt}, and potentially adverse impacts on T_{mrt}, at this time of day. Therefore, for tree-based and combined interventions, adverse impacts on UTCI may begin to show locally (Figure 7 and Table 3). Limited effectiveness is also observed for scenarios GV and VGS.1. Although these scenarios show statistically significant cooling of T_a of up to −0.2 K locally, potentially adverse impacts on T_{mrt} are estimated, particularly for scenario VGS.1; hence, no effective regulation UTCI and thus OTC is estimated for these GI types (Figure 7).

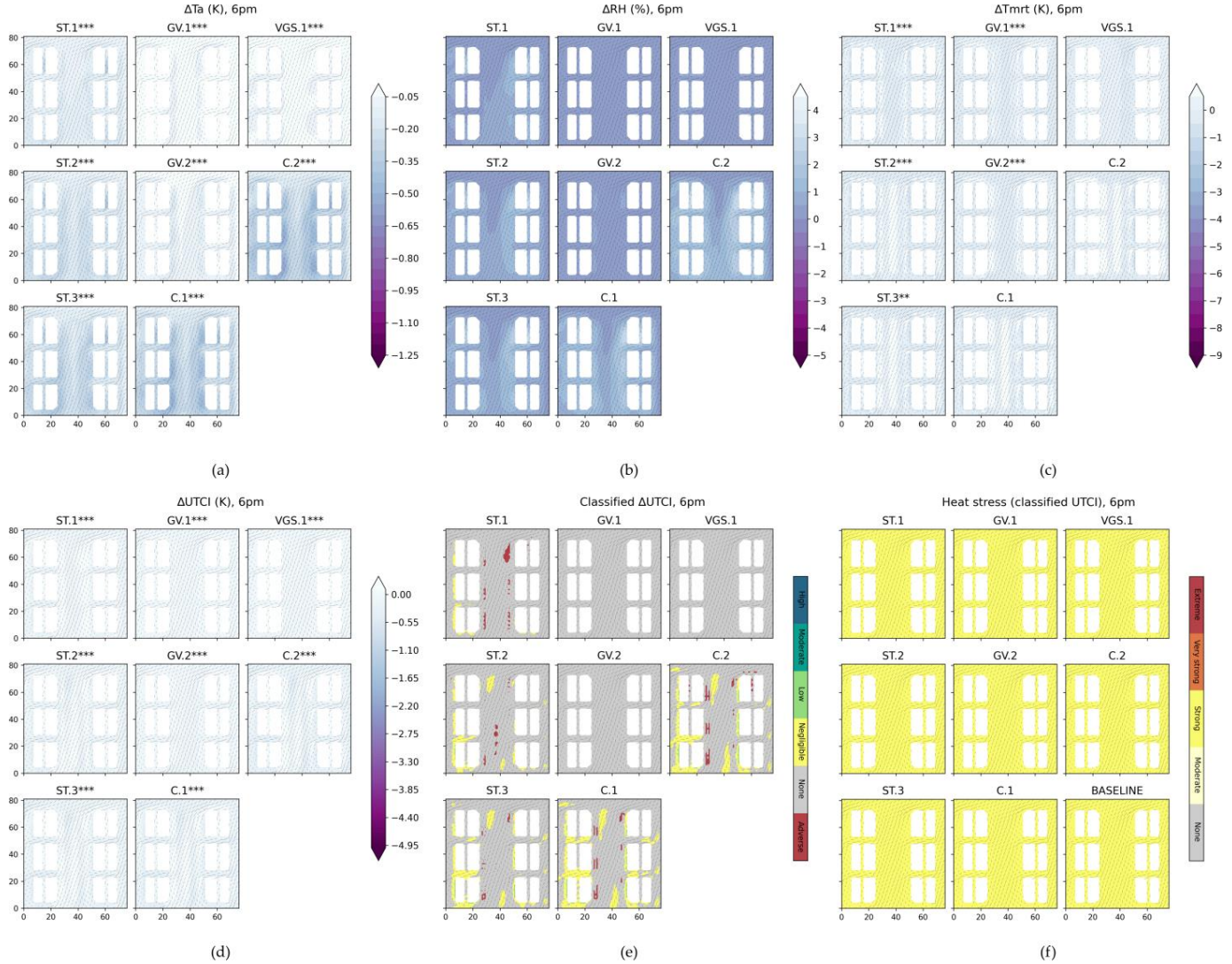

Figure 7. Simulation results at the pedestrian level for 6 p.m.: (**a**) local cooling potential (K); (**b**) changes in relative humidity (%); (**c**) difference in T_{mrt} (K); (**d**) local regulation of OTC; (**e**) classified local regulation of OTC; (**f**) heat stress. Prevailing wind speed and wind direction are shown as a Quiver plot. Please refer to Figure 4 for a description of the classes and significances. ***, highly significant ($p < 0.001$); non-significant otherwise ($p > 0.05$); **, very significant ($p < 0.01$).

Compared to tree-based scenarios, combined interventions seemingly have somewhat higher average and local T_a cooling potential and also show higher differences in UTCI (Table 3). However, at best, this translates to low contributions to UTCI regulation, limited primarily to the immediate adjacency of western building faces. Moreover, potentially

adverse impacts on T_{mrt} and hence OTC are also estimated for these scenarios, which, e.g., in the case of GV.2, may not be observed to that extent individually.

4. Discussion

The presented case study modeled the impacts of selected GI on T_a, RH, T_{mrt}, and UTCI as an indicator for OTC in order to assess the effectiveness of selected greening interventions for heat mitigation, and thus as a means to strengthen resilience towards climate change impacts in humid tropical cities. As outlined previously, the choice of GI under investigation was motivated primarily by its potential effectiveness, i.e., resulting in the choice of tree elements. However, local experiential knowledge on the feasibility of implementing specific types of GI and stakeholder preferences towards GI speaking towards the local cultural background were also considered in this choice [54].

Overall, it was shown that all types of GI interventions may provide certain cooling benefits with respect to T_a. There is also a significant impact of GI density on cooling delivery. Perhaps unsurprisingly, but confirming the results found in urban areas with various climatic conditions, tree-based interventions are associated with the highest predicted cooling effects [7,16]. The planting of street trees, as suggested in scenario ST.1, is already seen to have a significant cooling effect, which is most pronounced from around noon to late afternoon [20]. The planting of additional trees, particularly large deciduous trees with cylinder-shaped tree crowns, as proposed in scenarios ST.2 and ST.3, may result in the formation of a well-pronounced local cool island spanning large parts of the central collector road. This is in line with studies suggesting that deciduous trees, as well as trees with cylinder-shaped tree crowns, are particularly suited to adjust microclimatic conditions by cooling [77]. The impact of density on cooling becomes evident, as at 3 p.m., the average cooling potential of ST.2 compared to ST.1 is about 1.85-fold, and maximum cooling about 2.14-fold. A further increase in tree density, realized specifically as a double row planting pattern in scenario ST.3, was found to further amplify cooling, in line with the literature [21,22]. Thus, under local microclimatic conditions, achieving higher tree densities should provide more pronounced cooling impacts. The assessed maximum tree-based T_a cooling potential of 1.3 K is also in line with the previously modeled maximum daytime cooling potential of 1.5 K in shallow street canyons [78]. Moreover, despite low wind speeds, a higher cooling of T_a can be identified for downwind locations, as observed in [20], most noticeably along the central road's sidewalks. Here, e.g., for ST.1, local impacts appear to be 1.5–2-fold higher downwind compared to leeward (Figure 8).

Diurnal heat stress under simulated microclimatic conditions was determined to be strong to extreme except for morning conditions. Hence, any decrease in UTCI is considered positive for OTC, and it was found that tree-based cooling may contribute to the regulation of OTC during most times of day, with maximum domain-average reductions of UTCI between about −1.0 K (ST.1) and −1.9 K (ST.3). This is likely due to the increase in latent heat fluxes through evapotranspiration [69], and despite an associated increase in RH, which, from a physiological and biophysical perspective, should worsen heat stress due to a decrease in sweat evaporation [66,67]. However, particularly at high temperatures, the influence of RH on OTC-related health outcomes may be limited [67], and thermal discomfort may be driven particularly by air temperature [79].

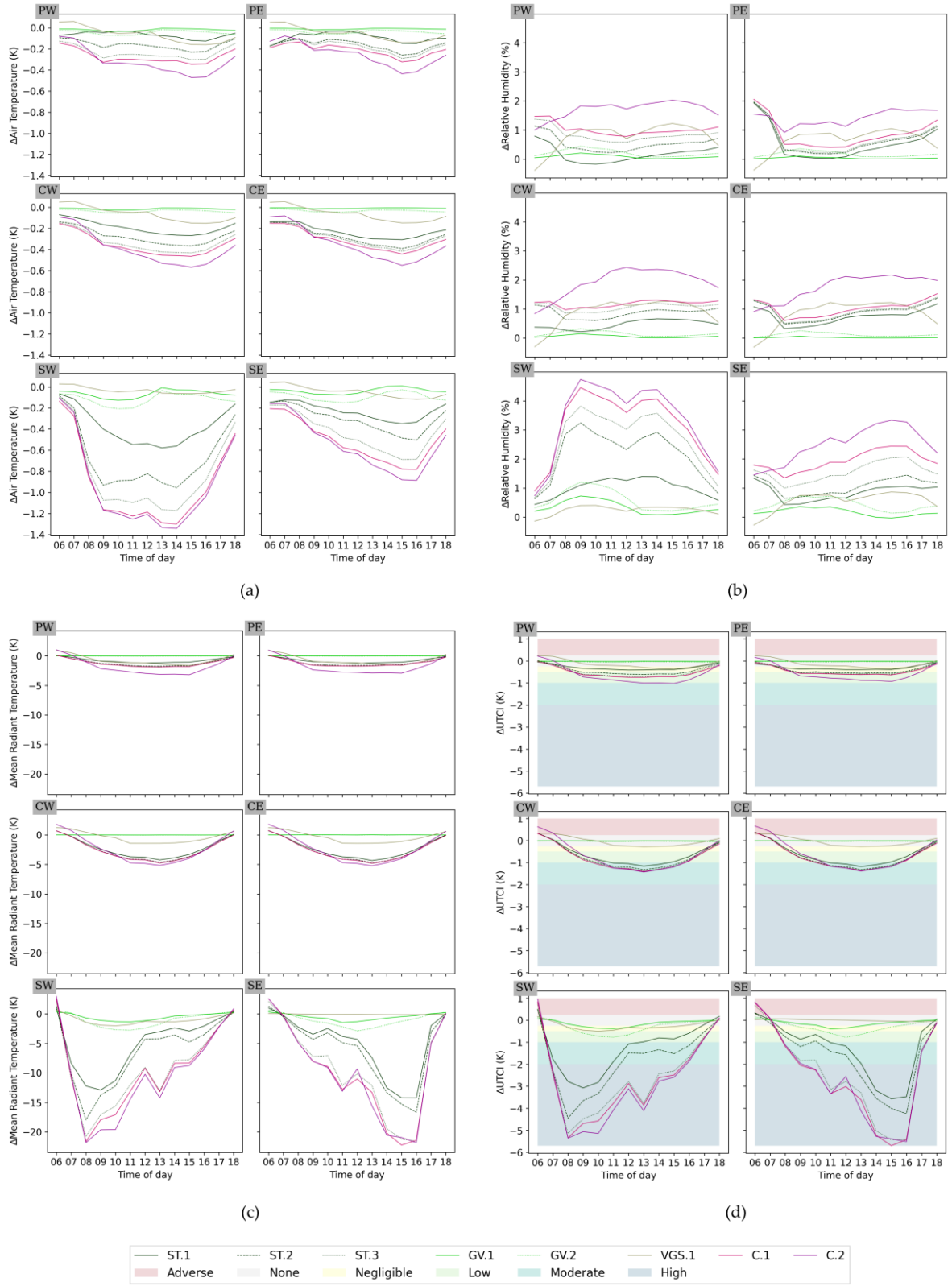

Figure 8. Simulated differences to baseline at chosen observer locations over time of day: PW (parking lot, western side), PE (parking lot, eastern side), CW (courtyard, western side), CE (courtyard, eastern side), SW (sidewalk, western side), and SE (sidewalk, eastern side). (**a**) Difference in air temperature (K); (**b**) difference in relative humidity (%); (**c**) difference in T_{mrt} (K); (**d**) difference in UTCI (K). Shaded areas refer to classified impact on UTCI, from adverse to high.

The higher impacts of trees on UTCI of about −4.0 K (ST.1) to −5.0 K (ST.2, ST.3) under trees themselves emphasize the importance of tree shade, or more generally, shading, for the regulation of T_{mrt} and thus OTC. The mean radiant temperature is an important meteorological parameter governing a human's energy balance [80–82], and as exemplified in Figure 3, the mean radiant temperature and UTCI, and thus OTC, are closely associated. Within tree-shaded areas, due to the blocking and absorption of incoming shortwave solar radiation, the mean radiant temperature may be decreased by about −20.0 K (Figure 8), thereby considerably improving shade-associated OTC. However, higher-density tree-based and combined interventions may also have more widespread beneficial impacts on T_{mrt} at the domain level. Consequently, tree-based interventions may help reduce pedestrian-level heat stress; therefore, increasing the number of street trees to provide shade and evaporative cooling may constitute a core element of locally adapted best practices or greening strategies for climate change adaptation with respect to urban heat, particularly within wider, shallow street canyons.

However, it has also been shown that at certain times of day, tree-based cooling does not translate into OTC improvements, potentially due to T_a cooling being counteracted by increasing RH, thereby limiting GI effectiveness [82]. Moreover, potentially adverse impacts through an increase of T_{mrt} and thus UTCI may be observed. This may be due to the trapping of outgoing longwave radiation below tree canopies and the subsequent accumulation of heat due to the blocking of ventilation [37,78]. This underlines the importance of tree species choice, planting configurations, e.g., optimized spacing between trees, and proper consideration of local wind patterns in the planning of greening interventions to retain urban ventilation [16,81–83]. Accordingly, in the scenarios considered, tree plantings follow priority locations for wide, shallow street canyons, in line with recommendations in the literature [3]. Under local conditions, this is important as wind speeds are typically low.

In addition to trees, a particular focus of this case study was on assessing the cooling performance of decidedly small GI elements, i.e., GV and VGS, as these elements may provide alternatives to stakeholders confronted with limited spatial potential. It has been shown that individually, these types of GI also provide significant T_a cooling, but at much lower magnitudes compared to tree-based interventions, and to a more limited spatial extent. Despite their overall small effects on T_a, GVs may provide certain benefits in terms of T_{mrt} and thus UTCI regulation, particularly when implemented in a higher density. Similar to trees, this is likely attributable to the increase in latent heat flux through evapotranspiration and a change in surface material and albedo affecting surface temperature, surface heat absorption, and thus radiant load [84]. VGSs were also found to potentially contribute to the regulation of UTCI. Again, this is likely due to evapotranspirative cooling and a modification of radiant load by a change in albedo, thus decreasing T_{mrt} [85]. However, the benefits of VGSs remain highly local and were found to be limited mainly to near proximity of greened building facades.

Then again, locally, the synergistic effects of combined GI implementation became apparent. For example, at 12 p.m. and 3 p.m., UTCI is more strongly reduced in parking lots under scenario C.2 than in either scenario ST.3, C.1, or VGS.1. Hence, adaptation strategies may aim at combining GI elements, thereby utilizing cooling impacts of GI synergistically, maximizing benefits for OTC regulation, and potentially compensating trade-offs, e.g., in terms of temporal patterns of delivered benefits, as exemplified by GVs and VGSs. Simultaneous greening interventions may also provide further synergies or trade-offs with respect to other ecosystem services, e.g., air filtration. It has been shown that depending on the street canyon orientation and morphology, larger and denser trees may lead to increased pollutant concentrations as well as reduced dispersion of pollution. Therefore, simultaneous close-to-source greening, e.g., in the form of green verges, hedges, or bushes, may not only support cooling but also increase deposition [86]. For example, in the elaborated scenarios, the choice of longer grass is expected to support such co-benefits. Likewise, although VGSs were found to have rather limited effectiveness in mitigating heat at the pedestrian level, they were also found to present viable options for the improvement

of air quality [87]. Additionally, green facades may have benefits for controlling building temperatures [28,29], which, however, were not assessed. Nonetheless, in the development of adaptation strategies, such potential co-benefits should be considered. It needs to be noted, though, that GI-associated increases in RH within hot, humid climates may also affect building energy balances negatively, e.g., by increasing energy usage for indoor cooling [82,88], prompting a careful evaluation of planned interventions.

It must also be emphasized that despite significant cooling benefits of the modeled interventions and associated diurnal OTC regulation, even comparatively high impacts on UTCI, with a reduction of about −2.1 K at the domain level, are not sufficient to lower heat stress to objective comfort levels. Although greenery has been found to be most effective for OTC regulation [32], additional measures, such as shading through changes in urban geometry and variation of building heights, or the use of alternative surface materials, may be considered to further improve OTC. Further investigations should also focus on subjective perceptions of OTC in the local context, particularly as an objective assessment of OTC may be insufficient as it may differ from subjective OTC, e.g., based on acclimatization and psychological adaptation [82,89,90].

Finally, further limitations and uncertainties of this case study need to be acknowledged. Regarding the former, it needs to be noted that only hot and muggy conditions were simulated, with air temperatures ranging from about 26.5 °C to 39.5 °C, high relative humidity of 45% to 96%, lack of low and medium cloud cover, and low wind speeds (Table 2). Such conditions are rather unfavorable meteorological conditions, resulting in comparatively high heat stress, as thermal discomfort is driven by high shortwave solar radiation driving mean radiant temperature, high air temperature, high relative humidity, and lack of wind [10]. It is acknowledged that assessed heat stress under baseline conditions, as well as impacts of GI, may vary considerably depending on seasonality and weather, and thus actual air temperature, relative humidity, and solar radiation in line with cloud cover. However, the modeled microclimate is considered typical for SEA humid tropical cities with high solar radiation, high humidity, and mostly low wind speeds year-round [35,43], and is therefore also seen to provide representative insights into the effectiveness of GI for conditions under which heat mitigation is urgently needed.

Further limitations are grounded in the limited spatial setting that has been modeled. The case study area is characterized by blocks of dense urban built-up adjacent to a central collector road, thus forming a wide, shallow street canyon as a central feature that is associated with specific thermal challenges. In this regard, the modeled spatial setting has been chosen, as it is considered representative of the wider planned urban expansion for Huế. Although the modeled interventions suggest potential for cooling and OTC regulation, GI impacts may vary considerably depending on urban morphology [82], for instance, regarding street width, street orientation and vegetation affecting wind flow, built-up density and height mediating radiant load, e.g., through a variation of sky view factor, or through diverse ground and surface materials used. Therefore, these findings may be cautiously applicable to similar spatial settings in SEA cities with comparable climatic conditions, particularly regarding the beneficial daytime impacts of tree shade. However, a more universal transferability of findings to other climatic settings, and urban morphologies different from wide, shallow street canyons, is limited: in a comparison of air temperature in Ho Chi Minh City across urban morphologies, differences of up to 2 K were found between spatial settings [33].

Uncertainty stems particularly from simulation accuracy. The overall fit of simulated air temperature and relative humidity to measured values is found to be good for the case study area [61–64], and RSME for T_a and RH are mostly within a similar range compared to [82]. However, the estimated mean bias error indicates, on average, an underestimation of air temperature by about 1.5 °C, and of relative humidity by about 7.5%. In this regard, in contrast to T_a and RH, a direct evaluation of the accuracy of simulated UTCI could not be conducted, as the mean radiant temperature could not be measured or obtained for validation, mainly due to equipment used as a function of available resources. However,

with respect to the mean radiant temperature as an important determinant of OTC, ENVI-met has been reported to account for direct, diffuse, and reflected shortwave radiation, and was found to be most accurate in a set of tools for modeling the longwave radiation field [91]. In an evaluation study for the city of Hong Kong, ENVI-met-simulated T_{mrt} was found to generally show very high agreement with measured values and low error magnitudes, with mean bias error of about 1.3 °C [92], whereas in a hot, Mediterranean climate, the accuracy of simulated mean radiant temperature has been described as reasonable, particularly within shaded locations, and an evaluation of UTCI accuracy showed reasonable agreement to measured values, with a mean bias error of 0.49 °C in shaded locations [93]. Therefore, with T_a, RH, and T_{mrt} potentially being underestimated by ENVI-met, it needs to be acknowledged that actual UTCI and thus heat stress may be higher than modeled, although the impacts of shading on OTC should be reasonably captured. Further uncertainty may arise from the sensitivity of OTC indices to changes in RH, with UTCI showing lower sensitivity to changes in relative humidity than to air temperature under local climatic conditions [94]. Nonetheless, UTCI was found to sufficiently represent human physiology, although it may be unsuitable for depicting all people and activities [94].

5. Conclusions

Using ENVI-met, this case study assessed the potential effectiveness of selected GI for heat adaptation in a humid tropical SEA city along a qualitative and a quantitative dimension. It is in such cities where urban heat mitigation is urgently needed in light of urbanization pressures and climate change, but where knowledge gaps, particularly for Vietnam, remain. In addressing this gap, and to support local heat mitigation and climate change adaptation action, pedestrian-level impacts of different types of GI on air temperature, relative humidity, mean radiant temperature, and UTCI as indicators for OTC were modeled and evaluated for a wide, shallow street canyon in the city of Huế, Vietnam. This chosen urban setting is considered representative of urban expansion projects in the city. In summary, it was found that pedestrian-level GI impacts are governed by GI choice (quality) and density (quantity). Regarding the qualitative dimension, tree-based interventions are seemingly most effective in providing daytime cooling and regulation of OTC, but may be associated with potentially adverse impacts on OTC in daytime margin hours and potentially overnight. However, at a lower level, decidedly small GI elements, i.e., green verges and, to a lesser extent, green facades, were found to help improve OTC, at least locally during certain times of day. Regarding the quantitative dimension, density dependence was found for tree-based interventions and green verges, with higher densities being associated with higher impacts. It was also assessed that the simultaneous implementation of different types of GI may allow harvesting the highest benefits for heat mitigation and that, furthermore, synergistic and added cooling may alleviate certain trade-offs of the investigated GI types. Combined implementation of GI may also allow for additional co-benefits.

It needs to be noted that in the modeled urban setting, no scenario could achieve a reduction of heat stress to objective comfort levels. Hence, additional measures for a more pronounced regulation of heat stress need to be identified. Further avenues of research include a more specific investigation on balancing GI-specific, OTC-related tradeoffs through combined implementations of GI, on the effectiveness of GI within other types of locally relevant urban morphologies, and on subjective perceptions of heat stress under local conditions.

Author Contributions: Conceptualization, S.S. and J.J.; data curation, J.J.; formal analysis, S.S. and J.J.; investigation, L.D.H.N., Y.V., T.B.M.H. and J.J.; methodology, S.S. and J.J.; validation, J.J.; visualization, S.S. and J.J.; writing—original draft, S.S., L.S. and J.J.; writing—review and editing, S.S. and L.S. All authors have read and agreed to the published version of the manuscript.

Funding: This research was funded by the German Federal Ministry of Education and Research, grant number 01LE1910A1, and by the CLEARING HOUSE (Collaborative Learning in Research,

Information-Sharing and Governance on How Urban Tree-Based Solutions Support Sino-European Urban Futures) Horizon 2020 project, grant number 821242.

Data Availability Statement: Dataset available on request from the authors.

Acknowledgments: We thank the Vietnamese project partners from the Thừa Thiên Huế Institute for Development Studies and the Faculty of Architecture of the University of Sciences/Huế University (HUSC) for their valuable contributions and cooperation.

Conflicts of Interest: The authors declare no conflicts of interest.

References

1. Asian Development Bank. *Viet Nam Environment and Climate Change Assessment*; Asian Development Bank: Manila, Philippines, 2013.
2. The World Bank Group and Asian Development Bank. *Climate Risk Country Profile: Vietnam*; World Bank Publications: Washington, DC, USA, 2021.
3. Norton, B.A.; Coutts, A.M.; Livesley, S.J.; Harris, R.J.; Hunter, A.M.; Williams, N.S.G. Planning for cooler cities: A framework to prioritise green infrastructure to mitigate high temperatures in urban landscapes. *Landsc. Urban Plan.* **2015**, *134*, 127–138. [CrossRef]
4. Endreny, T.A. Strategically growing the urban forest will improve our world. *Nat. Commun.* **2018**, *9*, 1160. [CrossRef] [PubMed]
5. Graça, M.; Cruz, S.; Monteiro, A.; Neset, T.-S. Designing urban green spaces for climate adaptation: A critical review of research outputs. *Urban Clim.* **2022**, *42*, 101126. [CrossRef]
6. Koc, C.B.; Osmond, P.; Peters, A. Evaluating the cooling effects of green infrastructure: A systematic review of methods, indicators and data sources. *Sol. Energy* **2018**, *166*, 486–508.
7. Livesley, S.J. The Urban Forest and Ecosystem Services: Impacts on Urban Water, Heat, and Pollution Cycles at the Tree, Street, and City Scale. *J. Environ. Qual.* **2016**, *45*, 119–124. [CrossRef] [PubMed]
8. Bowler, D.E.; Buyung-Ali, L.; Knight, T.M.; Pullin, A.S. Urban greening to cool towns and cities: A systematic review of the empirical evidence. *Landsc. Urban Plan.* **2010**, *97*, 147–155. [CrossRef]
9. Peng, Z.; Bardhan, R.; Ellard, C.; Steemers, K. Urban climate walk: A stop-and-go assessment of the dynamic thermal sensation and perception in two waterfront districts in Rome, Italy. *Build. Environ.* **2022**, *221*, 109267. [CrossRef]
10. Li, J.; Niu, J.; Mak, C.M.; Huang, T.; Xie, Y. Exploration of applicability of UTCI and thermally comfortable sun and wind conditions outdoors in a subtropical city of Hong Kong. *Sustain. Cities Soc.* **2020**, *52*, 101793. [CrossRef]
11. Nikolopoulou, M. Outdoor thermal comfort. *Front. Biosci. (Schol. Ed.)* **2011**, *3*, 1552–1568. [CrossRef] [PubMed]
12. Park, S.; Tuller, S.E.; Jo, M. Application of Universal Thermal Climate Index (UTCI) for microclimatic analysis in urban thermal environments. *Landsc. Urban Sci.* **2014**, *125*, 146–155. [CrossRef]
13. Xie, Y.; Huang, T.; Li, J.; Liu, J.; Niu, J.; Mak, C.M.; Lin, Z. Evaluation of a multi-nodal thermal regulation model for assessment of outdoor thermal comfort: Sensitivity to wind speed and solar radiation. *Build. Environ.* **2018**, *132*, 45–56. [CrossRef]
14. Jamei, E.; Ossen, D.R.; Seyedmahmoudian, M.; Sandanayake, M.; Stojcevski, A.; Horan, B. Urban design parameters for heat mitigation in tropics. *Renew. Sust. Energ. Rev.* **2020**, *134*, 110362. [CrossRef]
15. Aghamolaei, R.; Azizi, M.M.; Aminzadeh, B.; O'Donnell, J. A comprehensive review of outdoor thermal comfort in urban areas: Effective parameters and approaches. *Energy Environ.* **2022**, *34*, 2204–2227. [CrossRef]
16. Fu, J.; Dupre, K.; Tavares, S.; King, D.; Banhalmi-Zakar, Z. Optimized greenery configuration to mitigate urban heat: A decade systematic review. *Front. Archit. Res.* **2022**, *11*, 466–491. [CrossRef]
17. Kong, F.; Yin, H.; James, P.; Hutyra, L.; He, H.S. Effects of spatial pattern of greenspace on urban cooling in a large metropolitan area of eastern China. *Landsc. Urban Plan.* **2014**, *128*, 35–47. [CrossRef]
18. Segura, R.; Krayenhoff, E.; Martilli, A.; Badia, A.; Estruch, C.; Ventura, S.; Villalba, G. How do street trees affect urban temperatures and radiation exchange? Observations and numerical evaluation in a highly compact city. *Urban Clim.* **2022**, *46*, 101288. [CrossRef]
19. Baró, F.; Calderón-Argelich, A.; Langemeyer, J.; Connolly, J. Under one canopy? Assessing the distributional environmental justice implications of street tree benefits in Barcelona. *Environ. Sci. Policy* **2019**, *102*, 54–64. [CrossRef] [PubMed]
20. Tan, Z.; Ka-Lun Lau, K.; Ng, E. Planning strategies for roadside tree planting and outdoor comfort enhancement in subtropical high-density urban areas. *Build. Environ.* **2017**, *120*, 93–109. [CrossRef]
21. Atwa, S.; Ibrahim, M.G.; Murata, R. Evaluation of plantation design methodology to improve the human thermal comfort in hot-arid climatic responsive open spaces. *Sustain. Cities Soc.* **2020**, *59*, 102198. [CrossRef]
22. Zhao, Q.; Sailor, D.J.; Wentz, E.A. Impact of tree locations and arrangements on outdoor microclimates and human thermal comfort in an urban residential environment. *Urban For. Urban Green.* **2018**, *32*, 81–91. [CrossRef]
23. Djekić, J.P.; Mitković, P.B.; Dinić Branković, M.; Igić, M.Z.; Djekić, P.S.; Mitković, M.P. The Study of Effects of Greenery on Temperature Reduction in Urban Areas. *Therm. Sci.* **2018**, *22*, S989–S1000. [CrossRef]
24. Aboelata, A. Vegetation in different street orientations of aspect ratio (H/W 1:1) to mitigate UHI and reduce buildings' energy in arid climate. *Build. Environ.* **2020**, *172*, 106712. [CrossRef]
25. Tsoka, S.; Tsikaloudaki, A.; Theodosiou, T. Analyzing the ENVI-met microclimate model's performance and assessing cool materials and urban vegetation applications–A review. *Sustain. Cities Soc.* **2018**, *43*, 55–76. [CrossRef]

26. Bartesaghi-Koc, C.; Osmond, P.; Peters, A. Quantifying the seasonal cooling capacity of 'green infrastructure types' (GITs): An approach to assess and mitigate surface urban heat island in Sydney, Australia. *Landsc. Urban Plan.* **2020**, *203*, 103893. [CrossRef]
27. Chen, Y.; Zheng, B.; Hu, Y. Numerical Simulation of Local Climate Zone Cooling Achieved through Modification of Trees, Albedo and Green Roofs—A Case Study of Changsha, China. *Sustainability* **2020**, *12*, 2752. [CrossRef]
28. Jänicke, B.; Meier, F.; Hoelscher, M.-T.; Scherer, D. Evaluating the Effects of Façade Greening on Human Bioclimate in a Complex Urban Environment. *Adv. Meteorol.* **2014**, *2015*, 747259. [CrossRef]
29. Zölch, T.; Maderspacher, J.; Wamsler, C.; Pauleit, S. Using green infrastructure for urban climate-proofing: An evaluation of heat mitigation measures at the micro-scale. *Urban For. Urban Green.* **2016**, *20*, 305–316. [CrossRef]
30. Acero, J.A.; Koh, E.J.Y.; Li, X.; Ruefenacht, L.A.; Pignatta, G.; Norford, L.K. Thermal impact of the orientation and height of vertical greenery on pedestrians in a tropical area. *Build. Simul.* **2019**, *12*, 973–984. [CrossRef]
31. Buyantuyev, A.; Wu, J. Urban heat islands and landscape heterogeneity: Linking spatiotemporal variations in surface temperatures to land-cover and socioeconomic patterns. *Landsc. Ecol.* **2010**, *25*, 17–33. [CrossRef]
32. Huynh, C.; Eckert, R. Reducing Heat and Improving Thermal Comfort through Urban Design—A Case Study in Ho Chi Minh City. *Int. J. Environ. Sci. Dev.* **2012**, *3*, 480–485. [CrossRef]
33. Dang, H.T.; Pitts, A. Urban Morphology and Outdoor Microclimate around the "Shophouse" Dwellings in Ho Chi Minh City, Vietnam. *Buildings* **2020**, *10*, 40. [CrossRef]
34. Ngo, H.N.D.; Motoasca, E.; Versele, A.; Pham, H.C.; Breesch, H. Effect of neighbourhood courtyard design on the outdoor thermal comfort in a tropical city. *IOP Conf. Ser. Earth Environ. Sci.* **2022**, *1078*, 012035. [CrossRef]
35. Abdollahzadeh, N.; Biloria, N. Outdoor thermal comfort: Analyzing the impact of urban configurations on the thermal performance of street canyons in the humid subtropical climate of Sydney. *Front. Archit. Res.* **2021**, *10*, 394–409. [CrossRef]
36. Abdulateef, M.F.; Al-Alwan, H.A.S. The effectiveness of urban green infrastructure in reducing surface urban heat island. *Ain Shams Eng. J.* **2022**, *13*, 101526. [CrossRef]
37. Gál, T.; Mahó, S.I.; Skarbit, N.; Unger, J. Numerical modelling for analysis of the effect of different urban green spaces on urban heat load patterns in the present and in the future. *Comput. Environ. Urban Syst.* **2021**, *87*, 101600. [CrossRef]
38. Hwang, Y.H.; Lum, Q.J.G.; Chan, Y.K.D. Micro-scale thermal performance of tropical urban parks in Singapore. *Build. Environ.* **2015**, *94 Pt 2*, 467–476. [CrossRef]
39. Lin, B.-S.; Lin, C.-T. Preliminary study of the influence of the spatial arrangement of urban parks on local temperature reduction. *Urban For. Urban Green.* **2016**, *20*, 348–357. [CrossRef]
40. ENVI-met GmbH. *ENVI-met*; Version 5.0.3; Windows; ENVI-met GmbH: Essen, Germany, 2022.
41. Emmanuel, R.; Loconsole, A. Green infrastructure as an adaptation approach to tackling urban overheating in the Glasgow Clyde Valley Region, UK. *Landsc. Urban Plan.* **2015**, *138*, 71–86. [CrossRef]
42. Bruse, M.; Fleer, H. Simulating surface–plant–air interactions inside urban environments with a three dimensional numerical model. *Environ. Model. Softw.* **1998**, *13*, 373–384. [CrossRef]
43. Fong, C.S.; Aghamohammadi, N.; Ramakreshan, L.; Sulaiman, N.M.; Mohammadi, P. Holistic recommendations for future outdoor thermal comfort assessment in tropical Southeast Asia: A critical appraisal. *Sustain. Cities Soc.* **2019**, *46*, 101428. [CrossRef]
44. Dang, T.N.; Seposo, X.T.; Duc, N.H.C.; Thang, T.B.; An, D.D.; Hang, L.T.M.; Long, T.T.; Loan, B.T.H.; Honda, Y. Characterizing the relationship between temperature and mortality in tropical and subtropical cities: A distributed lag non-linear model analysis in Hue, Viet Nam, 2009–2013. *Glob. Health Action* **2016**, *9*, 28738. [CrossRef] [PubMed]
45. Nguyen, Q.P. Urban expansion and compulsory land acquisition in Hue, Vietnam: Challenges and ways towards fair urbanization. *LANDac* **2017**, *Policy Brief 05*, 1–8.
46. Peel, M.C.; Finlayson, B.L.; McMahon, T.A. Updated world map of the Köppen-Geiger climate classification. *Hydrol. Earth Syst. Sci.* **2007**, *11*, 1633–1644. [CrossRef]
47. Standing Committee of the National Assembly. *Resolution 1264/NQ-UBTVQH14 on 27 April 2021: Adjustment of the Administrative Geography of Administrative Units at the District Level and on the Ordering and Establishment of Wards in Hue City, Thua Thien Hue Province*; Socialist Republic of Vietnam: Hanoi, Vietnam, 2021.
48. Thua Thien Hue Province's Statistical Agency. *Statistical Yearbook of Thua Thien Hue Province 2021*; Thua Thien Hue Province's Statistical Agency: Hue, Vietnam, 2022.
49. Linh, N.H.K.; Tung, P.G.; Chuong, H.V.; Ngoc, N.B.; Phuong, T.T. The Application of Geographical Information Systems and the Analytic Hierarchy Process in Selecting Sustainable Areas for Urban Green Spaces: A Case Study in Hue City, Vietnam. *Climate* **2022**, *10*, 82. [CrossRef]
50. Rösler, K.; Konopatzki, P.; Jache, J.; Hoang, T.B.M.; Nguyen, D.H.L.; Scheuer, S.; Sumfleth, L.; Stolpe, F.; Haase, D. *Status Quo Report: Nature-Based Solutions in the City of Hue*; GreenCityLabHue: Berlin, Germany, 2020; Available online: https://www.greencitylabhue.com/wp-content/uploads/2020/07/Status-quo-report_NBS-in-Hue-City__2020-2-1.pdf (accessed on 1 January 2024).
51. CDC Stock Co. *Điều Chỉnh Quy Hoạch Chi Tiết Xây Dựng Khu Đô Thị Mới An Cựu Bản Đồ Quy Hoạch Kiến Trúc Cảnh Quan*; CDC Stock Co.: Hue, Vietnam, 2019.
52. Croce, S.; Vettorato, D. Urban surface uses for climate resilient and sustainable cities: A catalogue of solutions. *Sustain. Cities Soc.* **2021**, *75*, 103313. [CrossRef]

53. Mayrand, F.; Clergeau, P. Green Roofs and Green Walls for Biodiversity Conservation: A Contribution to Urban Connectivity? *Sustainability* **2018**, *10*, 985. [CrossRef]
54. Jache, J.; Scheuer, S.; Stolpe, F.; Sumfleth, L.; Dao, T.M.; Hoang, T.B.M.; Vo, Y.; Nguyen, D.H.L.; Zschiesche, M.; Haase, D. *GreenCityLabHuế: Nature-Based Solutions to Strengthen Climate Resilience of Urban Regions in Central Vietnam*; Final Report for the Definition Phase of the Joint Research Project; GreenCityLabHue: Berlin, Germany, 2021; Available online: https://www.greencitylabhue.com/wp-content/uploads/2021/04/GreenCityLabHue__final-project-report__2021.pdf (accessed on 1 January 2024).
55. ESRI. *ArcGIS Pro*; Version 3.0.1; ESRI: Redlands, CA, USA, 2022.
56. Shuhaimi, N.; Zaid, S.; Esfandiari, M.; Lou, E.; Mahyuddin, N. The impact of vertical greenery system on building thermal performance in tropical climates. *J. Build. Eng.* **2022**, *45*, 103429. [CrossRef]
57. Peng, L.; Jiang, Z.; Yang, X.; He, Y.; Xu, T.; Chen, S. Cooling effects of block-scale facade greening and their relationship with urban form. *Build. Environ.* **2020**, *169*, 106552. [CrossRef]
58. Robert McNeel & Associates. *Rhinoceros 3D*; Version 7; Robert McNeel & Associates: Seattle, WA, USA, 2020.
59. Papanikolaou, K.-T.; Liapi, K.; Sibetheros, I. Environmental Impact Assessment and Visualization of Rain-water Best Management Practices for Urban Blocks. An "architect-friendly" simulation model. In *Co-Creating the Future: Inclusion in and through Design Volume 2, Proceedings of the 40th Conference on Education and Research in Computer Aided Architectural Design in Europe, Ghent, Belgium, 13–16 September 2022*; Pak, B., Wurzer, G., Stouffs, R., Eds.; eCAADe and KU Leuven Faculty of Architecture: Ghent, Belgium, 2022; pp. 75–82.
60. Song, A.; di Nunzio, A.; Mackey, C.; Yang, J.; Roudsari, M.; Vasanthakumar, S. Dragonfly for Grasshopper. Available online: https://github.com/ladybug-tools/dragonfly-legacy (accessed on 6 June 2024).
61. Herath, H.M.P.I.K.; Halwatura, R.U.; Jayasinghe, G.Y. Evaluation of green infrastructure effects on tropical Sri Lankan urban context as an urban heat island adaptation strategy. *Urban For. Urban Green.* **2018**, *29*, 212–222. [CrossRef]
62. Ouyang, W.; Morakinyo, T.E.; Ren, C.; Ng, E. The cooling efficiency of variable greenery coverage ratios in different urban densities: A study in a subtropical climate. *Build. Environ.* **2020**, *174*, 106772. [CrossRef]
63. Cruz, J.A.; Blanco, A.C.; Garcia, J.J.; Santos, J.A.; Moscoso, A.D. Evaluation of the cooling effect of green and blue spaces on urban microclimate through numerical simulation: A case study of Iloilo River Esplanade, Philippines. *Sustain. Cities Soc.* **2021**, *74*, 103184. [CrossRef]
64. Cortes, A.; Rejuso, A.J.; Santos, J.A.; Blanco, A. Evaluating mitigation strategies for urban heat island in Mandaue City using ENVI-met. *J. Urban Manag.* **2022**, *11*, 97–106. [CrossRef]
65. Virtanen, P.; Gommers, R.; Oliphant, T.E.; Haberland, M.; Reddy, T.; Cournapeau, D.; Burovski, E.; Peterson, P.; Weckesser, W.; Bright, J.; et al. SciPy 1.0 Contributors. SciPy 1.0: Fundamental Algorithms for Scientific Computing in Python. *Nat. Methods* **2020**, *17*, 261–272. [CrossRef] [PubMed]
66. Sherwood, S.C. How Important Is Humidity in Heat Stress? *J. Geophys. Res. Atmos.* **2018**, *123*, 11808–11810. [CrossRef]
67. Baldwin, J.W.; Benmarhnia, T.; Ebi, K.L.; Jay, O.; Lutsko, N.J.; Vanos, J.K. Humidity's Role in Heat-Related Health Outcomes: A Heated Debate. *Environ. Health Perspect.* **2023**, *131*, 055001. [CrossRef] [PubMed]
68. Rahman, M.A.; Franceschi, E.; Pattnaik, N.; Moser-Reischl, A.; Hartmann, C.; Paeth, H.; Pretzsch, H.; Rötzer, T.; Pauleit, S. Spatial and temporal changes of outdoor thermal stress: Influence of urban land cover types. *Sci. Rep.* **2022**, *12*, 671. [CrossRef] [PubMed]
69. Rahman, M.A.; Moser, A.; Rötzer, T.; Pauleit, S. Within canopy temperature differences and cooling ability of Tilia cordata trees grown in urban conditions. *Build. Environ.* **2017**, *114*, 118–128. [CrossRef]
70. Fiala, D.; Havenith, G.; Bröde, P.; Kampmann, B.; Jendritzky, G. UTCI-Fiala multi-node model of human heat transfer and temperature regulation. *Int. J. Biometeorol.* **2012**, *56*, 429–441. [CrossRef] [PubMed]
71. Pantavou, K.; Lykoudis, S.; Nikolopoulou, M.; Tsiros, I.X. Thermal sensation and climate: A comparison of UTCI and PET thresholds in different climates. *Int. J. Biometeorol.* **2018**, *62*, 1695–1708. [CrossRef] [PubMed]
72. Zare, S.; Hasheminejad, N.; Shirvan, H.E.; Hemmatjo, R.; Sarebanzadeh, K.; Ahmadi, S. Comparing Universal Thermal Climate Index (UTCI) with selected thermal indices/environmental parameters during 12 months of the year. *Weather Clim. Extrem.* **2018**, *19*, 49–57. [CrossRef]
73. McGregor, G.R. Special issue: Universal Thermal Comfort Index (UTCI). *Int. J. Biometeorol.* **2012**, *56*, 419. [CrossRef] [PubMed]
74. Blazejczyk, K.; Epstein, Y.; Jendritzky, G.; Staiger, H.; Tinz, B. Comparison of UTCI to selected thermal indices. *Int. J. Biometeorol.* **2012**, *56*, 515–535. [CrossRef] [PubMed]
75. Wilcoxon, F. Individual comparisons by ranking methods. *Biom. Bull.* **1945**, *1*, 80–83. [CrossRef]
76. Guerri, G.; Crisci, A.; Morabito, M. Urban microclimate simulations based on GIS data to mitigate thermal hot-spots: Tree design scenarios in an industrial area of Florence. *Build. Environ.* **2023**, *245*, 110854. [CrossRef]
77. Milošević, D.; Bajšanski, I.; Savić, S. Influence of changing trees locations on thermal comfort on street parking lot and footways. *Urban For. Urban Green.* **2017**, *23*, 113–124. [CrossRef]
78. Coutts, A.; White, E.; Tapper, N.; Beringer, J.; Livesley, S. Temperature and human thermal comfort effects of street trees across three contrasting street canyon environments. *Theor. Appl. Climatol.* **2016**, *124*, 55–68. [CrossRef]
79. Wei, D.; Yang, L.; Bao, Z.; Lu, Y.; Yang, H. Variations in outdoor thermal comfort in an urban park in the hot-summer and cold-winter region of China. *Sustain. Cities Soc.* **2022**, *77*, 103535. [CrossRef]

80. Gál, C.V.; Kántor, N. Modeling mean radiant temperature in outdoor spaces, A comparative numerical simulation and validation study. *Urban Clim.* **2020**, *32*, 100571. [CrossRef]
81. Kong, F.; Yan, W.; Zheng, G.; Yin, H.; Cavan, G.; Zhan, W.; Zhang, N.; Cheng, L. Retrieval of three-dimensional tree canopy and shade using terrestrial laser scanning (TLS) data to analyze the cooling effect of vegetation. *Agric. For. Meteorol.* **2016**, *217*, 22–34. [CrossRef]
82. Meili, N.; Acero, J.A.; Peleg, N.; Manoli, G.; Burlando, P.; Fatichi, S. Vegetation cover and plant-trait effects on outdoor thermal comfort in a tropical city. *Build. Environ.* **2021**, *195*, 107733. [CrossRef]
83. Lai, S.; Zhao, Y.; Fan, Y.; Ge, J. Characteristics of daytime land surface temperature in wind corridor: A case study of a hot summer and warm winter city. *J. Build. Eng.* **2021**, *44*, 103370. [CrossRef]
84. Lindberg, F.; Onomura, S.; Grimmond, C.S.B. Influence of ground surface characteristics on the mean radiant temperature in urban areas. *Int. J. Biometeorol.* **2016**, *60*, 1439–1452. [CrossRef] [PubMed]
85. Kim, E.S.; Yun, S.H.; Lee, D.K.; Kim, N.Y.; Piao, Z.G.; Kim, S.H.; Park, S. Quantifying outdoor cooling effects of vertical greening system on mean radiant temperature. *Dev. Built Environ.* **2023**, *15*, 100211. [CrossRef]
86. Janhäll, S. Review on urban vegetation and particle air pollution—Deposition and dispersion. *Atmos. Environ.* **2015**, *105*, 130–137. [CrossRef]
87. Tomson, M.; Kumar, P.; Barwise, Y.; Perez, P.; Forehead, H.; French, K.; Morawska, L.; Watts, J. Green infrastructure for air quality improvement in street canyons. *Environ. Int.* **2021**, *146*, 106288. [CrossRef] [PubMed]
88. Fonseca, J.; Schlueter, A. Daily enthalpy gradients and the effects of climate change on the thermal energy demand of buildings in the United States. *Appl. Energy* **2020**, *262*, 114458. [CrossRef]
89. Silva, T.J.V.; Hirashima, S.Q.S. Predicting urban thermal comfort from calibrated UTCI assessment scale—A case study in Belo Horizonte city, southeastern Brazil. *Urban Clim.* **2021**, *36*, 100652. [CrossRef]
90. Nikolopoulou, M.; Steemers, K. Thermal comfort and psychological adaptation as a guide for designing urban spaces. *Energy Build.* **2003**, *35*, 95–101. [CrossRef]
91. Naboni, E.; Meloni, M.; Mackey, C.; Kaempf, J. The Simulation of Mean Radiant Temperature in Outdoor Conditions: A review of Software Tools Capabilities. In Proceedings of the Building Simulation 2019: 16th Conference of IBPSA, Rome, Italy, 2–4 September 2019; pp. 3234–3241.
92. Sinsel, T.; Simon, H.; Ouyang, W.; dos Santos Gusson, C.; Shinzato, P.; Bruse, M. Implementation and evaluation of mean radiant temperature schemes in the microclimate model ENVI-met. *Urban Clim.* **2022**, *45*, 101279. [CrossRef]
93. Aleksandrowicz, O.; Saroglou, T.; Pearlmutter, D. Evaluation of summer mean radiant temperature simulation in ENVI-met in a hot Mediterranean climate. *Build. Environ.* **2023**, *245*, 110881. [CrossRef]
94. Simpson, C.H.; Brousse, O.; Ebi, K.L.; Heaviside, C. Commonly used indices disagree about the effect of moisture on heat stress. *NPJ Clim. Atmos. Sci.* **2023**, *6*, 78. [CrossRef]